

DTIC FILE COPY

2

NAVAL POSTGRADUATE SCHOOL Monterey, California

AD-A219 792



THESIS

DTIC
ELECTE
MAR 28 1990
S E D

NAVAL AIRBORNE ESM SYSTEMS ANALYSIS

by

Oswaldo R. Rosero

September 1989

Thesis Advisor:

Robert L. Partelow

Co-Advisor:

Thomas H. Hoivik

Approved for public release; distribution unlimited

90 03 23 192

REPORT DOCUMENTATION PAGE

1a. REPORT SECURITY CLASSIFICATION UNCLASSIFIED			1b. RESTRICTIVE MARKINGS NONE		
2a. SECURITY CLASSIFICATION AUTHORITY N.A.			3. DISTRIBUTION/AVAILABILITY OF REPORT Approved for public release, distribution unlimited.		
2b. DECLASSIFICATION/DOWNGRADING SCHEDULE N.A.			5. MONITORING ORGANIZATION REPORT NUMBER(S) N.A.		
4. PERFORMING ORGANIZATION REPORT NUMBER(S) N.A.			7a. NAME OF MONITORING ORGANIZATION		
6a. NAME OF PERFORMING ORGANIZATION Naval Postgraduate School		6b. OFFICE SYMBOL (if applicable) Code 3A	7b. ADDRESS (City, State, and ZIP Code)		
6c. ADDRESS (City, State, and ZIP Code) Monterey CA. 93943			9. PROCUREMENT INSTRUMENT IDENTIFICATION NUMBER		
8a. NAME OF FUNDING / SPONSORING ORGANIZATION		8b. OFFICE SYMBOL (if applicable)	10. SOURCE OF FUNDING NUMBERS		
8c. ADDRESS (City, State, and ZIP Code)		PROGRAM ELEMENT NO	PROJECT NO	TASK NO	WORK UNIT ACCESSION NO.
11. TITLE (Include Security Classification) Naval Airborne ESM Systems Analysis					
12. PERSONAL AUTHOR(S) Oswaldo R. Rosero					
13a. TYPE OF REPORT Thesis		13b. TIME COVERED FROM _____ TO _____		14. DATE OF REPORT (Year, Month, Day) September, 1989	
15. PAGE COUNT 146					
16. SUPPLEMENTARY NOTATION The views expressed in this thesis are those of the author and do not reflect the official policy or position of the Department of Defense or the U.S. Government					
17. COSATI CODES			18. SUBJECT TERMS (Continue on reverse if necessary and identify by block number)		
FIELD	GROUP	SUB-GROUP	Electronic Warfare, ESM, Superhet, IFM		
19. ABSTRACT (Continue on reverse if necessary and identify by block number) The purpose of this thesis is to evaluate naval airborne tactical Electronic Support Measures systems based on particular operational requirements of the Ecuadorian Navy. The analysis is based upon the formulation of a time dependent Probability of Intercept as a measure of effectiveness. The model includes common parameters involved in the Electronic Support Measures process and relates them with various Electronic Warfare receiver techniques available. This thesis recommends the best technological concepts available for each mission. RRH					
20. DISTRIBUTION/AVAILABILITY OF ABSTRACT <input checked="" type="checkbox"/> UNCLASSIFIED/UNLIMITED <input type="checkbox"/> SAME AS RPT <input type="checkbox"/> DTIC USERS			21. ABSTRACT SECURITY CLASSIFICATION UNCLASSIFIED		
22a. NAME OF RESPONSIBLE INDIVIDUAL Robert L. Partelow			22b. TELEPHONE (Include Area Code) (408) 646-2081		22c. OFFICE SYMBOL Code 62 Pw

Approved for public release, distribution unlimited

Naval Airborne ESM System Analysis

by

Oswaldo R. Rosero
Lieutenant j.g. Ecuadorian Navy
B.S. Ecuadorian Naval Academy, 1983

Submitted in partial fulfillment of the
requirements for the degree of

MASTER OF SCIENCE IN SYSTEMS ENGINEERING

from the

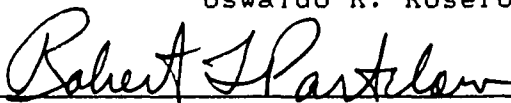
NAVAL POSTGRADUATE SCHOOL
September 1989

Author:

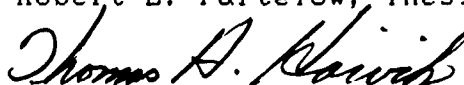


Oswaldo R. Rosero

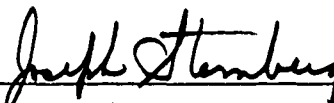
Approved by:



Robert L. Partelow, Thesis Advisor



Thomas H. Hoivik, CAPT. USN, Thesis Co-advisor



Joseph Sternberg, Chairman,
Electronic Warfare Academic Group

ABSTRACT

The purpose of this thesis is to evaluate naval airborne tactical Electronic Support Measures systems based on particular operational requirements of the Ecuadorian Navy. The analysis is based upon the formulation of a time dependent Probability of Intercept as measure of effectiveness. The model includes common parameters involved in the Electronic Support Measures process and relates them with various Electronic Warfare receiver techniques available. This thesis recommends the best technological concept available for each mission.

Accession For	
NTIS GRA&I	<input checked="" type="checkbox"/>
DTIC TAB	<input type="checkbox"/>
Unannounced	<input type="checkbox"/>
Justification	
By _____	
Distribution/	
Availability Codes	
Dist	Avail and/or Special
A-1	



ACKNOWLEDGMENT

The author wishes to thank the Ecuadorian Navy, the United States Navy and the Naval Postgraduate School for the education opportunity; Prof. Robert Partelow and Capt. Thomas Hoivik for their invaluable time and help; my parents because they taught me how to walk on life; and finally my wife Cecilia and my son Oswaldo Jr. because they knew how to light every moment, and they were always there when I needed them the most.

TABLE OF CONTENTS

I. INTRODUCTION	1
A. BACKGROUND	2
II. SCENARIO	5
A. THE GEOGRAPHICAL REGION	5
B. FRIENDLY FORCES	6
1. Close to Coast Engagements (up to 100 nm.)	7
2. Medium Range Engagements (100 to 200 nm.)	7
3. Long Range Engagements (> 200 nm.)	8
C. THE POSSIBLE THREAT	9
III. ESM AND THE PARAMETERS TO BE MEASURED	11
A. ENVIRONMENTAL ELECTRONIC DENSITY	11
B. PARAMETERS OF INTEREST	13
C. DYNAMIC RANGE AND SENSITIVITY	14
1. Dynamic Range	15
2. Receiver Sensitivity	15
D. GEOMETRICAL CONSIDERATIONS	23
E. PARAMETERS ACCURACY	29
IV. ESM MEASURES OF EFFECTIVENESS	33

A.	PROBABILITY OF DETECTION	34
B.	PROBABILITY OF COINCIDENCE	35
C.	PROBABILITY OF IDENTIFICATION	41
V.	ANALYSIS	50
A.	PROBABILITY OF DETECTION ANALYSIS	50
B.	PROBABILITY OF COINCIDENCE ANALYSIS	53
C.	PROBABILITY OF IDENTIFICATION ANALYSIS	57
D.	POI ANALYSIS	60
E.	SENSITIVE ANALYSIS OF WEIGHTING FACTORS	64
VI.	CONCLUSIONS	68
A.	GENERAL CONCLUSIONS	68
B.	SPECIFIC CONCLUSIONS	68
C.	OPERATIONAL CONCLUSIONS	69
VII.	RECOMENDATIONS	71
	APPENDIX A: SENSITIVITY REQUIREMENTS	72
	APPENDIX B: SETUP (SUPERHET)	79
	APPENDIX C: SETUP (IFM)	82
	APPENDIX D: PROBABILITY OF DETECTION (SUPERHET)	85

APPENDIX E: PROBABILITY OF DETECTION (IFM)	93
APPENDIX F: PROBABILITY OF IDENTIFICATION (SUPERHET) . .	102
APPENDIX G: PROBABILITY OF IDENTIFICATION (IFM)	112
APPENDIX H: PROBABILITY OF COINCIDENCE (SUPERHET)	122
APPENDIX I: PROBABILITY OF COINCIDENCE (IFM)	127
APPENDIX J: PROBABILITY OF INTERCEPT	132
LIST OF REFERENCES	135
DISTRIBUTION LIST	137

1. INTRODUCTION

The purpose of this thesis is to determine an optimum Naval Airborne Tactical Electronic Warfare System from selected components. Its characteristics of performance will be derived from particular mission requirements, generated from Ecuadorian naval tactical operational needs.

In history there are plenty of examples that confirm that a military action will better succeed if sufficient reconnaissance/surveillance has supported the final decision. In this particular case, an ESM system must provide sufficient and accurate information in order to locate the enemy and clarify the tactical situation, that is; what are the enemy forces disposition, strength, intentions, discretion, readiness, etc.?. In other words, the ESM receiver should collect data from all the emitters of interest, over a wide frequency spectrum, over large angular regions, and with sufficient sensitivity to improve detection ranges; then it must measure and process this information quickly and accurately for immediate use as a decision basis.

There are basically three different kinds of receivers available in a very mature technological state: a.) Crystal Video Receivers (CVR), b.) Instantaneous Frequency Measurement (IFM) and c.) Superheterodyne. The particular

characteristics of each one of them, will be analyzed to identify their applicability to Naval requirements.

A. BACKGROUND

In the past twenty years, there has been a growing interest among Third-World nations in strengthening the naval presence in oceanic areas of interest, justified by principles and policies of military strategy, and due to the natural growth or maturity achieved with time and experience.

The late sixties brought about challenging new weapons: the Sea skimming surface to surface missile (SSM's) , and the fast attack missile boat (FAMB's). As a result the concepts of Naval Warfare were shaken with the enormous changes that these two weapons represented to the traditional way of making war at sea.

Subsequently, both the FAMB's and the SSM's were proven in different actions around the world, and due to their successes many Navies have adopted them as the "pattern to follow", even though in many cases they were not wisely utilized, or were not used for those purposes for which both the missile or the FAMB were appropriate. There are many examples to cite, where countries have acquired FAMB's for purposes of patrolling their Exclusive Economic Zone but found them to be not cost-effective. In other cases, endurance and seakeeping capabilities of the FAMBs have been overestimated. The fact is that the presence of FAMB's

represents a threat to forces attempting to penetrate their defensive zones. Additionally, their cost of operation is much less than for a Destroyer or Frigate.

Ecuador is a particular case where FAMB's were bought in order to replace Second World War vintage destroyers, achieving at low cost a considerable power projection capability. This was not the best solution for two reasons:

First because of the geographical situation of that country, (located at the Northwestern part of South America and with a wide open sea in front of it) was not the best environment for missile boat operations since they are better used in restricted waters. And second, the large open ocean area, combined with the limited endurance and surveillance capabilities of the FAMB's, made it very impractical to search, locate, attack and destroy threats with the required level of success. As with bigger ships, the problem of searching and locating the enemy remains the key point for success at sea, and this is very difficult to solve with the limitations of the FAMB's. In any case, during the UNITAS operations held from 1984 to 1986 (in which the author participated), an experimental solution was operationally tested which consisted of combining a Surface Attack Group with a P-3C, where the aircraft carried the task of searching for and locating enemy forces and then vectoring the missile boats towards the threat until they reached missile launching position.

It may be important to note that operating with this combination gave very significant results in extending the effective operational radius of the FAMB's and their lethality, especially when engaging surface forces with limited air support. Clearly, the aircraft tasks were of extreme importance, and particularly the ESM tactics and techniques employed which were paramount to overall mission success. In addition to this, the aircraft enjoyed the advantage of its versatility which allowed it to selectively operate its active emitters, and thereby approach closer to the target (under certain conditions) for positive identification.

It is becoming evident that a cost-effective solution for improving ones own power projection capabilities is to outfit surveillance aircraft with appropriate ESM systems, and to develop the related tactics for their employment either alone or in combination with a Surface Attack Group. This thesis will analyze several airborne ESM System in order to satisfactorily accomplish the mission and operational requirements as stated above.

11. SCENARIO

The scenario considered by this thesis is that of a Naval aircraft in Electronic Warfare surveillance operations attempting to target an already classified enemy ship. The aircraft will have the support of an Surface Attack Group (SAG) for weapons delivery on the target.

The object of the ESM mission is to obtain and process sufficient and accurate ESM data. This is not a simple matter since many complex parameters are involved. Some parameters may not be improved without trading off the performance of the system in another area. Other parameters are under the enemy's control or are of random nature. This thesis is limited to a particular scenario, which is divided into three specific parts:

- The Geographical region,
- One's own forces and,
- The possible threat

A. THE GEOGRAPHICAL REGION

The Geographical region of interest is the Northwestern part of South America, (where Ecuador is located) from the coastline up to about 900 miles westward, and Northward to the Panama Canal. Historically, the extent of the region has

been justified by both national and hemispherical interests. Actually, Ecuador's national maritime interests are the protection of its Economic Exclusive Zone and maritime communication lines; and in the case of an hemispherical threat, the navies of this region will have to share the responsibilities for protection of vital maritime communication lines. In fact, the most recent UNITAS operations have underscored this point by increasing the joint exercises between the navies of Ecuador, Colombia, Venezuela, and the USA, on both the Atlantic and the Pacific sides of the Panama Canal. Ecuador possesses naval and aeronaval facilities along the Pacific coast and in the Galapagos Islands which are located 600 miles west of the continent.

B. FRIENDLY FORCES

The available forces will be mostly Missile Boats ranging upwards from 125 Tons to 800 Tons, equipped with ESM equipment on board. Actually, Ecuador possesses a missile force of 6 Corvettes and 6 fast attack missile boats. Since each different sized FAMB will have different endurance, it is necessary to deploy them wisely according to mission characteristics, scale of conflict and nature of the threat. In any case, during the crucial initial phases of the encounter, both surveillance and command and control requirements must be accomplished by the ESM aircraft in order

to achieve the required degrees of surprise and accuracy in the surface attack.

The main weapon chosen was the French Exocet MM38 and MM40 missiles with 21 and 40 nautical miles of range respectively.

As was stated above, the deployment of forces depends on complex own and enemy related factors. The following are examples of scenarios that might happen and how own forces would be arranged, according to range from the advanced bases available.

1. Close to Coast Engagements (up to 100 nm.)

It would be advisable to use mostly smaller FAMB's, with the size of the threat determining how many boats will be dispatched to achieve a power advantage.

2. Medium Range Engagements (100 to 200 nm.)

In this scenario, the general choice is to select larger FAMBs. However if enemy classification is obtained in time, it might be advisable to send a combination of FAMB's, with the smaller units closer to the target, thereby allowing simultaneously firing of the MM38 and MM40 missiles. With this deployment, one can exploit the proven advantages of relative Radar and ESM detection ranges, using the smaller FAMB's with their reduced radar cross sections to proceed closer to their targets.

3. Long Range Engagements (> 200 nm.)

Longer endurance units (Corvettes) will be required for this scenario, but the attack group must also include a sufficient number of FAMB's to counter the threat size.

Some scenario parameters evaluated as common to all the cases described above are:

a) The surveillance aircraft must detect, classify, identify and locate the enemy ship prior to further action; and additionally to this, it must vector and command the attack group properly until the point where Boats' commanders assume total control of the action.

b) A minimum of 2 attacking units will be required.

c) A minimum of 2 missiles will be fired at each target to increase the probability of hit.

d) After the attack has been made, the units will leave the area at full speed.

e) The surveillance aircraft will be used for evaluating the results of the attack, and/or collecting valuable information that might support conclusions about the outcome of the action or previous situation. Using this information it will allow:

1) Reengagement if the situation is favorable.

2) Relocation of additional ships if saturation of enemy's defenses is required,

or,

3) Launch of a second attack if the enemy's reaction has been weak and slow.

f) Prior to and during the attack, the deployed SAG will maintain a distance between units of about 5 to 15 miles for ESM triangulation, UHF communication purposes, and for fire power coverage.

All these courses of action are derived from the information obtained by electronic surveillance during the search and detection phase of the engagement.

C. THE POSSIBLE THREAT

The threat which this thesis analyzes, is a surface warship such of a destroyer or cruiser type, acting as a picket of a surface force, or as part of a surface action group, and having little or no airborne early warning support. Additionally, the ship will have an on-board helo for anti-surface operations.

The main weapons system for this ship consists of a medium range AA missile (30 to 40 nm.), a short range AA missile (10 nm.) and over-the-horizon surface to surface missiles.

In order to properly accomplish these tasks, this ship will have the following sensors:

- 1 Long range air search radar (frequency agility capable),

- 1 Medium range-low altitude air search radar,
- 1 Tactical surface search radar,
- 1 Navigation radar,
- 3 Fire control radars, and
- 1 Surface search radar on the helo.

III. ESM AND THE PARAMETERS TO BE MEASURED

A. ENVIRONMENTAL ELECTRONIC DENSITY

The environmental electronic density plays a key role in the design of the ESM system, since this density establishes some of the operational requirements under which the system will be developed.

For example, the number of emitters and their transmitting characteristics, their location relative to own receiver, the level of hostilities, and the type of mission to be accomplished by own forces, are among all the factors that outline the environment one will work with.

According to Ref.[5] the electromagnetic density for systems with sensitivity below -70 dBm is particularly altitude independent. This particular value deserves to be mentioned because we will refer back to it later when the ESM parameters are defined and analyzed within each System configuration.

From the model cited above, and using the formula for maximum unambiguous range, we can estimate the pulse density to be the following (pulses per second):

$$PRF = c/2 \cdot \text{range} \quad (2-1)$$

where:

PRF = Pulse repetition Frequency (pulses per second)

c = Speed of light

range= Maximum Unambiguous Range

The radars expected to be present are:

- | | | |
|----|----------------------------------|------------------------|
| a) | Long range search radar (aerial) | 300 Fp. (277nm.range) |
| b) | Medium range search (aerial) | 1012 Fp (80 nm.range) |
| c) | Tactical surface search | 1079 Fp. (75 nm.range) |
| d) | Navigation radar | 1620 Fp. (50 nm range) |
| e) | Fire control radars (3) | 2699 Fp. (30 nm range) |
| f) | Search radar (Helo) | 1000 Fp. (80 nm range) |

This makes a total of 13,108 Fp for each ship in the case where all the sensors are radiating. This number give us a good starting point for the analysis since, as stated above, we might expect to find more than one enemy ship in the zone, in addition, merchant ships will be in the area and at some stage we will also have to count own ships radars. Assuming that we will encounter a maximum of 10 ships with similar characteristics to those cited above, all transmitting their radars simultaneously, we will have a total Pulses per Second of 131,080 Fp (pps).

For the purposes of this thesis the airborne system will have a processing capability of about 300,000 pulses per second. in order to satisfy and exceed, within a sufficient level. the requirements imposed by the tactical situation.

B. PARAMETERS OF INTEREST

In order to create a decision basis, an ESM system must detect and process many parameters from the emitter, and the more parameters are obtained and successfully analyzed, the easier is to determine the emitter's identity.

Additionally, some ESM parameters are considered more valuable than others in a given situation; such as the Angle of Arrival (AOA) or the frequency characteristics of the intercepted signal, which contribute the most to emitter identification. Generally, the ESM receiver will be required to measure the following parameters from the emitter:

Angle of arrival (AOA),

Frequency (f),

Time of arrival (TOA),

Pulse width (PW), and

Pulse amplitude (PA).

These parameters have been intentionally ordered according to their importance to mission accomplishment (i.e., sorting and identification).

As can be found on the commercial market, ESM receivers range from detecting one to detecting all of the above parameters, but if emitter sorting, classification and identification are required (which is usually the case with naval ESM) a minimum of three parameters are needed.

A basic receiver scheme is independent of which parameters are being measures. For example:

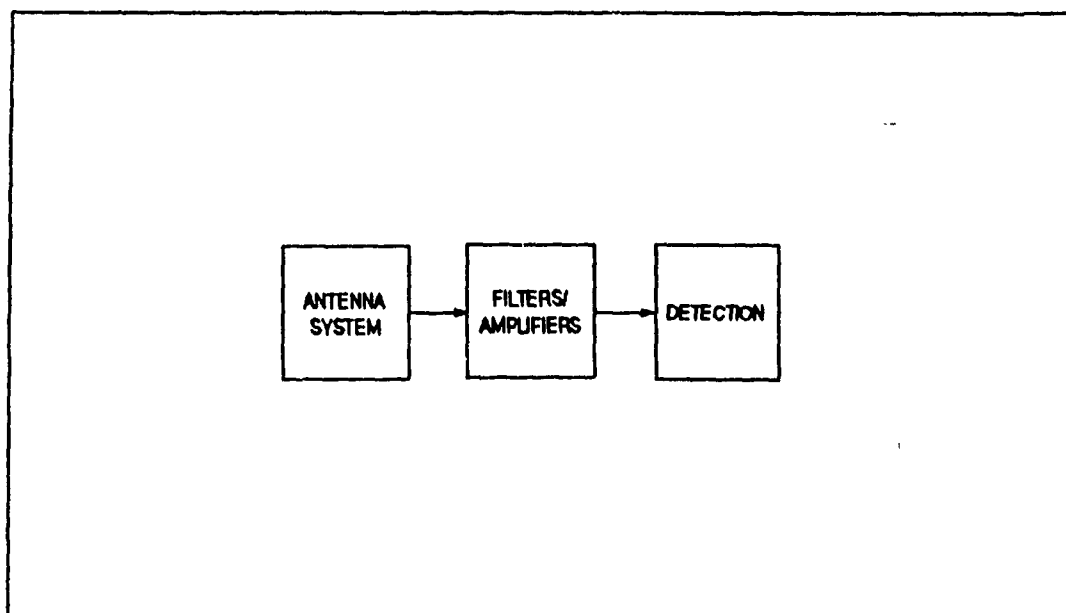


Fig. 1, Basic receiver system

C. DYNAMIC RANGE AND SENSITIVITY

Dynamic Range and Sensitivity are of extreme importance in ESM receiver design. If performance in both are poorly realized, the overall system performance will be seriously degraded. On the other hand, if good dynamic range and sensitivity are available at the receiver, then many parameters such as detection range, accuracy of the measurements, sorting capability, probability of detection, etc. will give the system and the user an advantageous decision basis. In the author's point of view, any design must first start by setting appropriate values for these two fundamental specifications.

1. Dynamic Range

The Dynamic Range defines the range of input power over which the receiver will work properly, generally expressed in decibels (dB). The lower limit of the dynamic range is the system's sensitivity, and the upper is defined in different manners, the most common being the one dB compression point. The input power is linearly related to the output power, but as the input power increases there is a certain limit where the output power loses its linear relationship and falls below the ideal. When the difference between the ideal linear receiver and the actual output power is 1 dB, then the value of the input power (at which the 1 dB difference occurs) is the upper limit of the required dynamic range.

If the input power goes above this limit, the receiver saturates, the gain is lowered, and spurious signals will appear at the Receiver's output. To cope with the expected range of the signals strengths, a Dynamic Range of at least 65 dB is required.

2. Receiver Sensitivity

The System's Sensitivity defines the weakest signal power that can be detected by the System and generate an output where the Signal to Noise ratio meets the minimum required.

As will be addressed later in the detectability problem, a certain minimum power level of the target emitter is also required to produce a detection at a given probability. The emitter's radiation power must compete inside the ESM receiver with the intrinsic thermal noise (internally generated) that represents the floor of the system. The sensitivity floor is a function of both noise power and signal to noise ratio (SNR).

The noise power (N) at the receiver's output is modeled by the well known following relationship that assumes a Gaussian noise (resistor) model:

$$N = k \cdot T_o \cdot B_n \cdot F_n \quad (3-1)$$

where:

$$k = 1.38 \cdot 10^{-23} \quad \text{Boltzman's constant}$$

T_o = Noise Temperature (in Kelvin)

B_n = Receiver noise Bandwidth (Hz.)

F_n = Receiver noise Figure

If we use $T = 290^\circ \text{ K}$, and express the power in milliwatts then:

$$N(\text{dBm}) = -174 \text{ dBm} + 10 \log_{10} (B_n) + 10 \log_{10} (F_n) \quad (3-2)$$

The receiver noise figure (F_n) relates the actual noise power output to the ideal receiver's output.

The effective noise bandwidth (B_n) becomes a very important consideration when instantaneous wideband receivers are used, therefore, even though a wide bandwidth might be available for interception at the receiver's front end, this does not represent directly the noise power available because when the signal reaches the detector, most of the original noise is filtered out by the narrow bandwidth of the video stage. This is referred to sometimes as "Processing Gain", and it is proportional to the ratio of the Acceptance Bandwidth (B_a) to the Video Bandwidth (B_v), where γ is the integration efficiency.

$$B_n = \frac{B_{rf}}{\left[\frac{B_{rf}}{2 B_v} \right]^\gamma} \quad (3-3)$$

γ varies from 0.5, (when the ratio B_{rf}/B_v is large) to about 0.8 or 0.9 for Superheterodyne receivers ($B_{rf}/B_v = 2$, approx.).

The signal received from the emitter is given by:

$$S = \frac{P_t \cdot G_t \cdot G_{sm} \cdot \lambda^2 \cdot g^2}{(4 \cdot \pi \cdot R)^2 \cdot L_{sm} \cdot L_t} \quad (3-4)$$

where:

P_t = Radar transmitter peak power (watts)
 G_t = Radar transmitter antenna gain
 G_{esm} = ESM receiver antenna gain
 λ = c/f ; Wavelength (meters)
 g = Multipath factor
 R = Range between radar and ESM receiver
 L_{esm} = ESM receiver losses
 L_t = Radar transmitter losses

The Signal to noise ratio will be defined by combining the previous three equations:

$$SNR = \frac{P_t \cdot G_t \cdot G_{esm} \cdot \lambda^2 \cdot g^2}{(4\pi R)^2 \cdot k \cdot T_o \cdot B_n \cdot F_n \cdot L_t \cdot L_{esm}} \quad (3-5)$$

Where B_n is in Hertz.

These two definitions, noise floor and SNR, are quite important because they represent the basis for the following system design. Two parameters directly related to the noise and SNR of the system are the maximum detection range and the probability of detection / false alarm.

The power advantage of the ESM receiver comes from its $1/R^2$ propagation loss versus the $1/R^4$ propagation loss for the radar.

In Fig. 1 we see the relationship between signal power received at the ESM and radar receivers in dBw as a function of range, showing a difference that increases with distance.

In appendix A, MATHCAD 2.0 is used for solving the equations and plotting the variations of signal power at reception, both at the Radar and at the ESM receiver, given their characteristics. Figure 2 shows the $1/R^2$ advantage of the ESM receiver which allows it (given the same range for Radar and ESM Receiver) the use of a lower sensitivity level; and if the sensitivity of the ESM receiver is enhanced from this value, a tremendous advantage in detection range is achieved. The Radar and ESM parameters involved in the following plots are:

Radar; Long Range Air Surveillance type,

Pt = 250 Kw. Transmitter Peak Power (Kw.)

Gt = 1585 Antenna Gain (mainlobe)

PW = $4.0 \cdot 10^{-6}$ s. Pulse Width

λ = 0.1 m Wavelength (meters)

Lt = 2 Transmitter losses

g = 1 Multipath factor

ht = 20 m Antenna height

ESM System:

Gesm = 1 ESM receiver Antenna Gain (Omni)

hesm = 1000 m ESM aircraft height

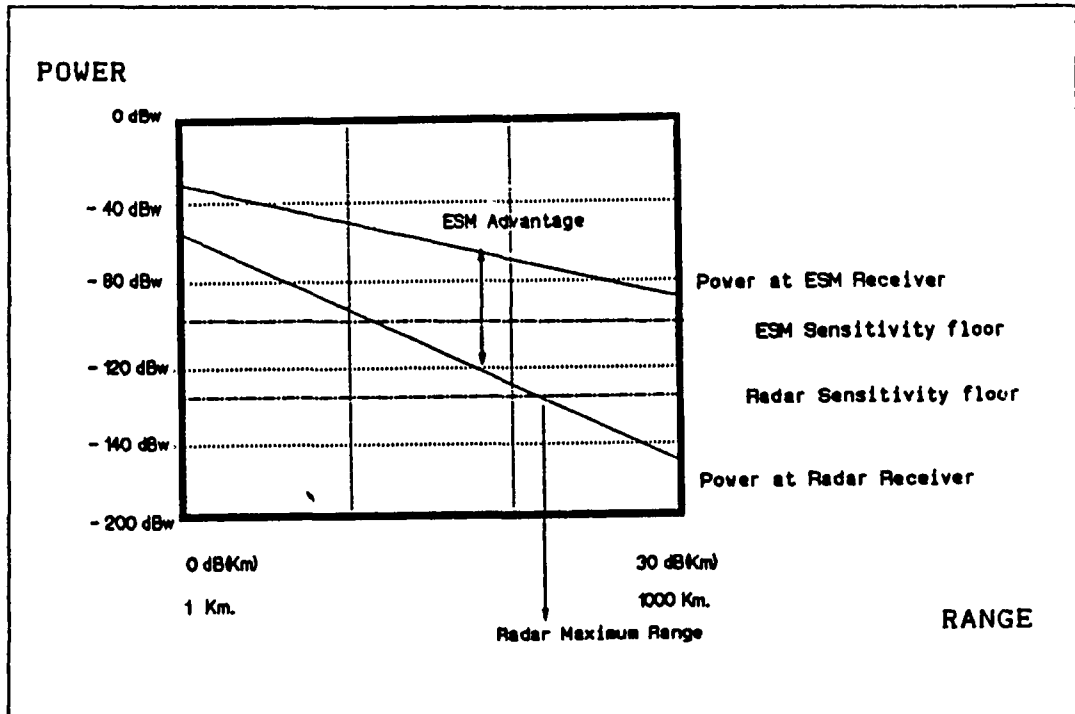


Fig. 2 Radar and ESM receiver propagation, in dB, for a particular radar.

The following step is to add more realistic data to the comparison by introducing the radar range equation to the effects of noise and the minimum signal to noise ratio required. For a specified radar design, the most important improvement is achieved if the SNR is set to the lowest possible level, therefore, if the SNR is defined as the independent variable of the equation, we can estimate the radar detection range. In this analysis, the SNR (minimum) of the radar is varied from 10 dB to 15.5 dB (10 to 35.5)

radar detection range. In this analysis, the SNR (minimum) of the radar is varied from 10 dB to 15.5 dB (10 to 35.5) which are values commonly employed by radar designers.

As indicated in Figure 3, using a conservative approach, the target has a 10 dB SNR at a maximum detection range of about 200 Km.. This suggests why it is important to gather basic data from a hostile emitter (peak power, antenna size and gain, pulse width, frequency, etc.), since it will allow E.W. planners to estimate radar performance and counter with the appropriate ESM equipment.

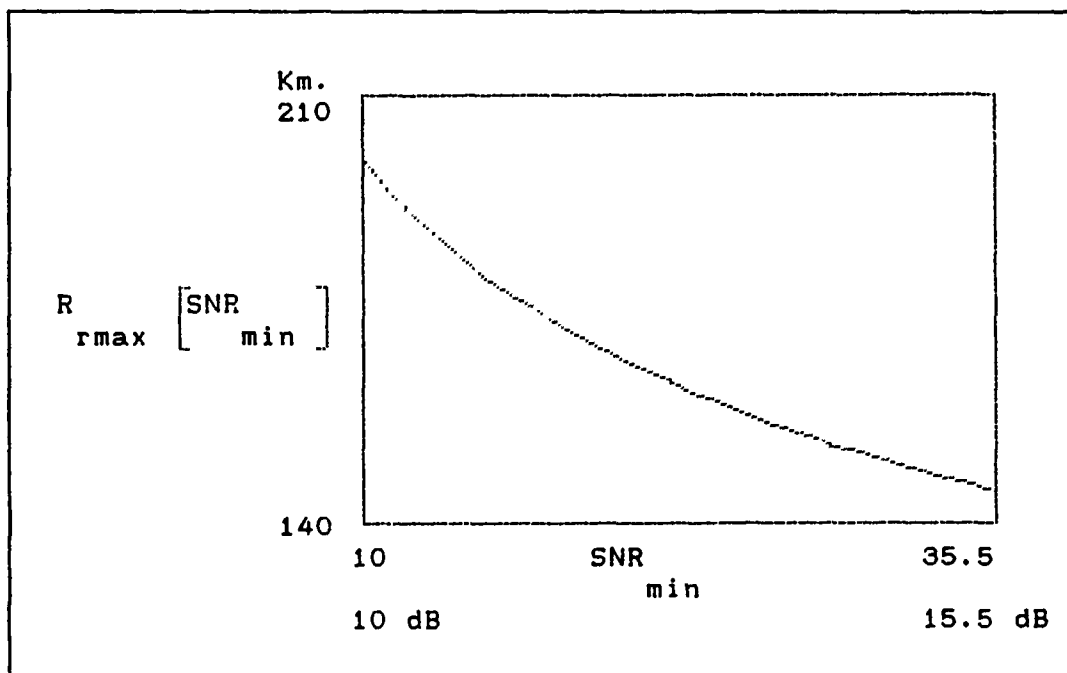


Fig. 3 Radar maximum detection range (R_{rmax}) as function of minimum signal to noise ratio (SNR_{min})

detection range is set as a function of the sensitivity and the sensitivity is varied over the range stated, the plot shown in Figure 4 is obtained.

From Figure 4 it can be concluded that for Sensitivities above -45 dBm, the ESM receiver performance is poor since we know that the maximum detection range of the Radar is about 200 Km.; but as the sensitivity drops to -50 dBm or below, the increment in ESM detection range increases rapidly. The best weapon that airborne naval ESM surveillance could make use of is its detection range advantage. Therefore, no receiver with sensitivities above -50 dBm will be considered appropriate for the purposes of this thesis and that automatically eliminates the use of CVRs for further evaluation.

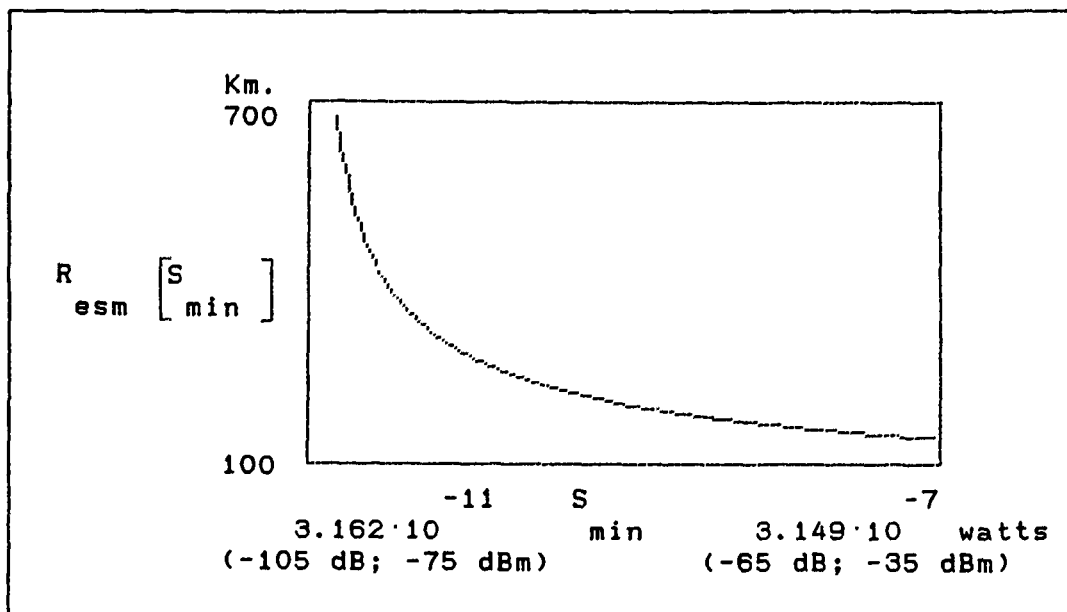


Fig 4. ESM performance in Range for detection

D. GEOMETRICAL CONSIDERATIONS

In developing a tactical ESM mission, it is important to ensure that flight altitude and detection range are defined together. To determine this relationship, there are three parameters to be considered:

a) First, given the emitter and aircraft altitudes, a radar horizon exists that physically limits microwave propagation. The following equation calculates the horizon limited range, dependent on Earth's sphericity and atmospheric refraction. This relationship is taken from [Ref. 4]:

$$R_{\text{hoz}} = 130.34 \cdot \left[(h_{\text{esm}})^{.5} + (h_{\text{t}})^{.5} \right] \quad (3-6)$$

where:

h_{t} = Radar height (in Km)

h_{esm} = ESM receiver height (in Km)

b) Second, we define a maximum ESM detection range (R_{esm}) dependent on ESM receiver and radar characteristics:

$$R_{\text{esm}} = \left[\frac{P_{\text{t}} \cdot G_{\text{t}} \cdot G_{\text{esm}} \cdot \lambda^2 \cdot g^2}{(4 \cdot \pi)^2 \cdot S_{\text{min}} \cdot L_{\text{t}} \cdot L_{\text{esm}}} \right]^{0.5} \quad (3-7)$$

If the aircraft's altitude is too low, the radar horizon becomes the limit for the maximum detection range.

In order to optimize the capability for searching and detecting, the flight height must be chosen such that the radar horizon equals the maximum ESM detection range:

(3-8)

$$130.34 \cdot \left[(h_{\text{esm}}(\text{Km}))^{0.5} + (h_t(\text{Km}))^{0.5} \right] = \left[\frac{P_t \cdot G_t \cdot G_{\text{esm}} \cdot \lambda^2 \cdot g^2}{(4 \cdot \pi)^2 \cdot S_{\text{min}} \cdot L_t \cdot L_{\text{esm}}} \right]^{0.5}$$

(3-9)

$$h_{\text{esm}}(\text{Km}) = \left[7.67 \cdot 10^{-6} \left[\frac{P_t \cdot G_t \cdot G_{\text{esm}} \cdot \lambda^2 \cdot g^2}{(4 \cdot \pi)^2 \cdot S_{\text{min}} \cdot L_t \cdot L_{\text{esm}}} \right]^{0.5} - h_t(\text{Km})^{0.5} \right]^2$$

This is a basis for later reference, and is simplified, not taking into account other factors that affect the performance of the system. This approach assumes the maximum detection range as the principal factor of interest but most of the time it is limited by the aircraft altitude (about 10 Km.).

As can be seen in the Figures 5 and 6 which plot the height for the radar side and main lobe detection, the altitudes required are relatively low for sensitivities above -65 dBm (300 m. for -65 dBm) against the side lobes, on the other hand if the main lobe gain is considered in the calculation, the height goes far above reasonable or operationally realistic numbers (above 1000 Km. for -75 dBm, and around 13 Km for -65 dBm).

c) Finally a most important consideration is grazing angle. If an aircraft is located at or below the tangential line of sight defined by the radar horizon, the performance of the radar emitter will be considerably degraded because of the low grazing angle of the emission over the earth's surface. This increases the sea clutter and diffraction effects that can produce a lot of scattering and fading on the radar signal during its propagation and reception. The use of this tangential line will define what will be called the ESM horizon slant range.

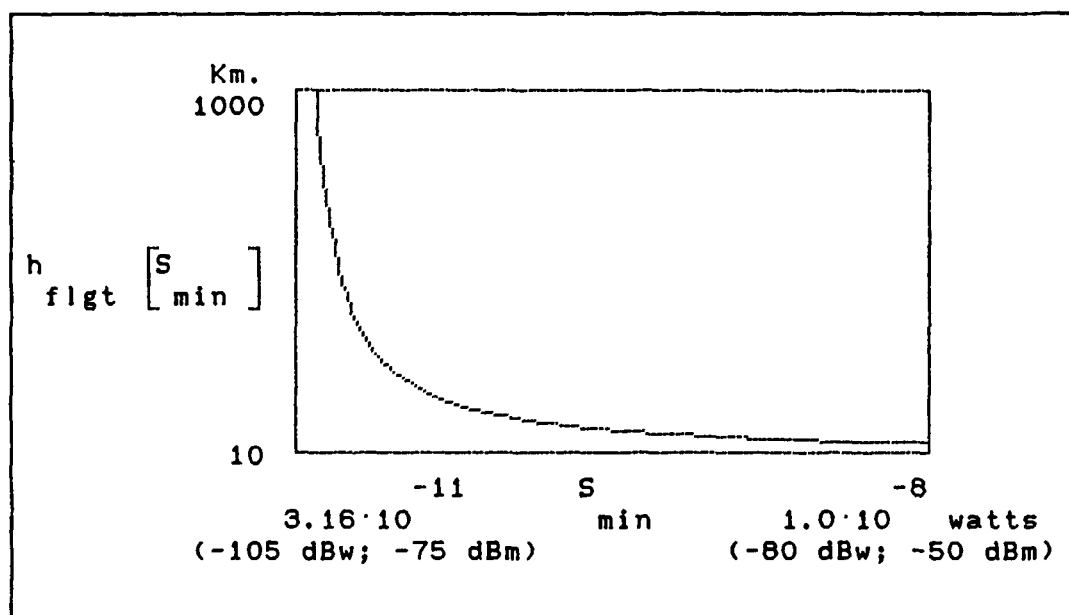


Fig. 5 Flight height for Main lobe detection

Additionally because of the round trip requirement it becomes very difficult for the Radar to perform in an acceptable way under such conditions. On the other hand, the

ESM receiver is not seriously affected by this phenomena because it will receive the direct ray without problems and

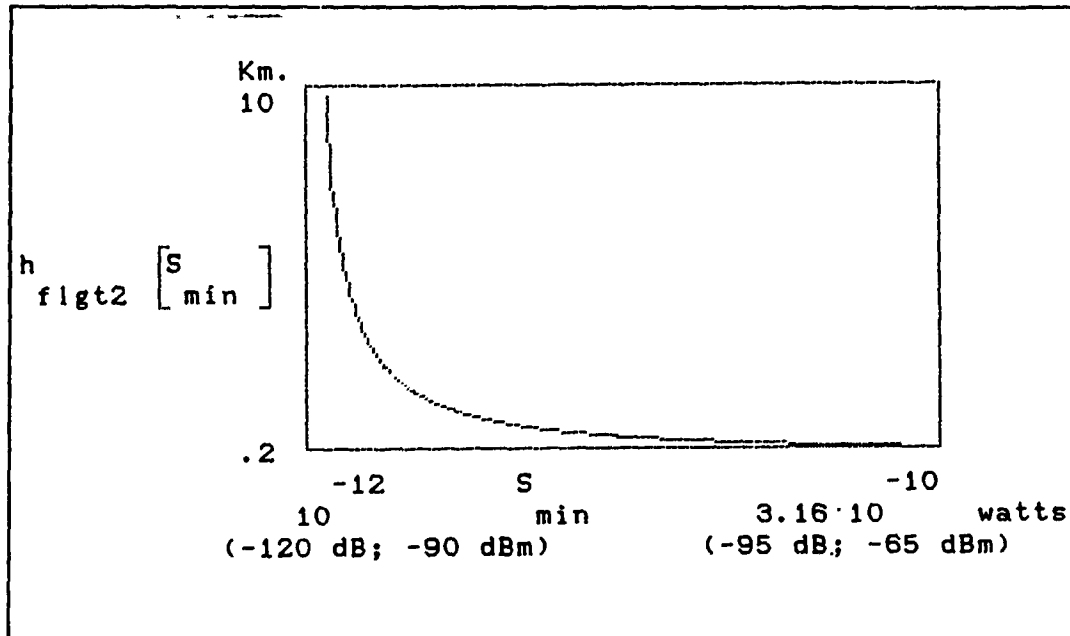


Fig. 6 Flight height for side lobes detection

with a relatively high power level. Ideally it would be preferred to always fly in this tangential approach. Then, once detection has occurred while flying towards the emitter, it must continuously lower its altitude trying to stay within the radar worst detection zone the maximum possible time. Within the scope of this thesis, the aircraft will be assumed to be flying at constant speed and altitude, since the purpose is to evaluate and analyze the variations of time and reception performance parameters in a simulated environment. However, further research should include the tangential flight path combined with of other ESM requirements such as signal

to noise ratio, or time of coincidences, probability to intercept vs. time, etc., to investigate additional performance improvements.

In Figures 7 and 8 we see the theoretical conditions of this tangential approach, which includes heights, ranges, main lobe and side lobes detection.

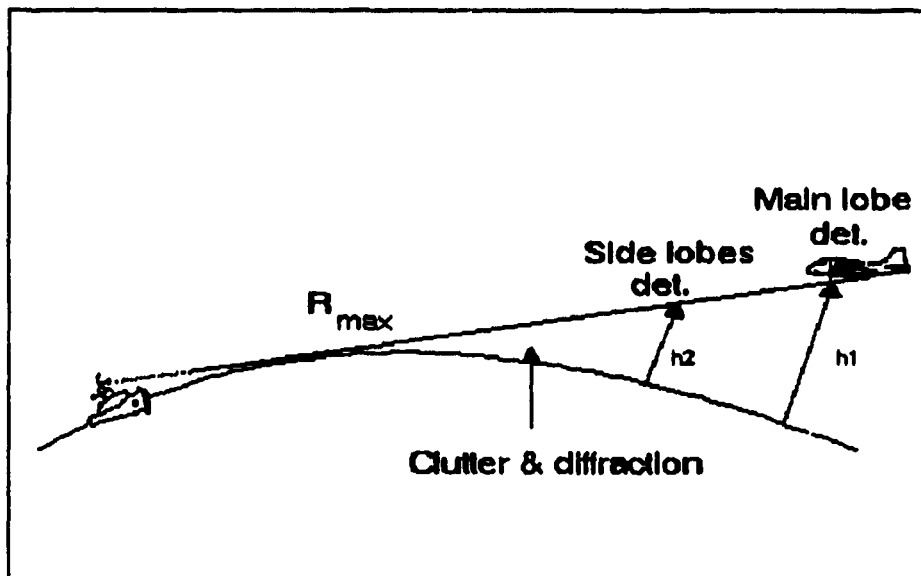


Fig. 7 Electronic Horizon slant range.

We can conclude at this stage, that the performance of an airborne ESM system initially depends on how far away it is able to search, therefore the flight height must be properly chosen in order to exploit the tangential approximation the longest time possible. Lowering the range improves the emitter side lobes interception by the ESM receiver but the altitude must be adjusted so that the smaller

range, indicated from the sensitivity standpoint, is just at the electronic horizon slant range. If the altitude is higher at the time this side lobes detection is achieved, we might well be inside the radar detection range in a region of better radar reception, having lost the detectability advantage of the ESM/Elint aircraft.

A sensitive analysis, (Appendix J) using MATHCAD demonstrated that the improvement of radar sidelobes detection is not as important as the ability to obtain the maximum information possible from the main lobe emission and this is a strong function of the maximum detection range.

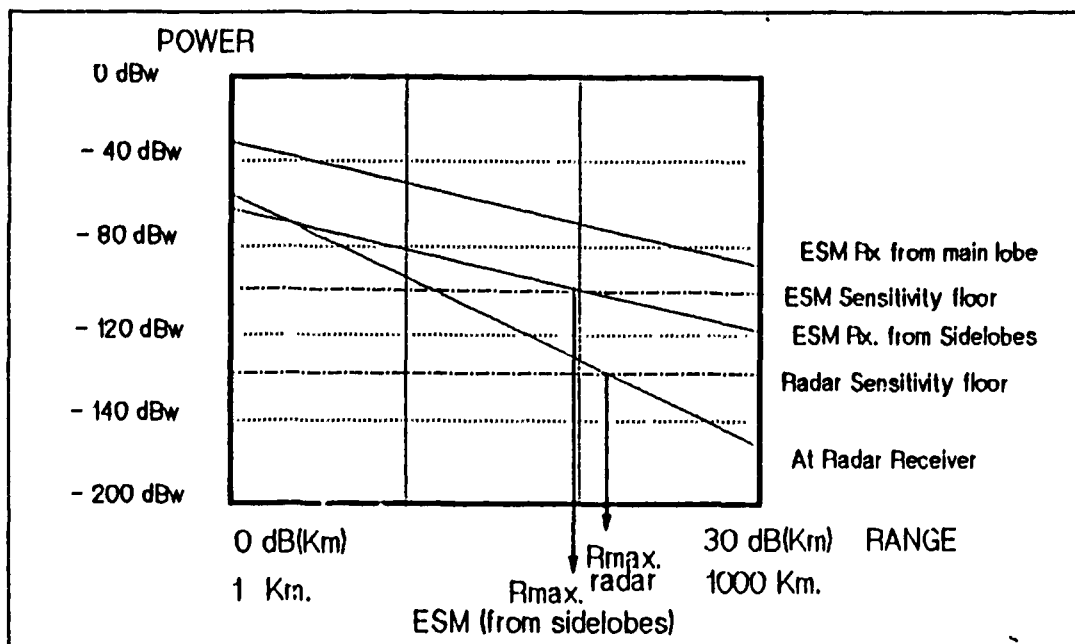


Fig. 8 Power availability at radar and ESM Rx. versus range

For the model, depicted in Figure 7, which represents a typical radar and an IFM receiver, detection of the sidelobes (which are 32 dB below the main lobe), occurs at ranges less than the radar maximum detection range. Perhaps a more sensitive ESM receiver should be considered if sensing the side lobes while avoiding radar detections is such a desirable objective. An improvement is obtainable with their higher sensitivity receivers, and it may be justifiable for an ESM system designer to evaluate this capability quantitatively.

E. PARAMETERS ACCURACY

The real accuracy of the ESM parameters of interest is obtained by statistical analysis of sample measurements, gathered experimentally, and is expressed in standard deviation form.

$$\sigma = \left[\frac{\Sigma (x_i - \bar{x})^2}{n} \right]^{0.5} \quad (3-10)$$

where:

n = Number of measurements taken

\bar{x} = parameter Sample mean

x_i = Sample data value

To improve the accuracy of the measurements, n should be large ($n > 30$). The quality of the ESM receiver system can be inferred if the difference term of the numerator is small and if the parameter sample mean is close to the source parameters.

According to Wiley [Ref. 2, p.135] the accuracy value, required for an acceptable measurement, ranges from 0.1% to 1%, which is the ratio of the standard deviation to the actual value of the parameter being measured. Ortiz [Ref. 9], and Giaquinto [Ref.10] in their respective works used accuracy requirement values of 0.1% for frequency measurement and 1% for both Pulse Repetition Interval (PRI) and Pulse Width (PW) measurements. These were reasonably chosen and correspond to values in commercially available receivers.

From Refs. 3, 4, 9, 10 and 12, the theoretical standard deviation errors for frequency, PRI, and PW (as functions of the Signal to Noise Ratio) for a Superhet receiver are respectively:

$$df = \left[\frac{3}{2 \cdot \pi^2 \cdot PW^3 \cdot B_n \cdot SNR} \right]^{0.5} ; \max = B_a \quad (3-11; 3-12)$$

where B_a is the receiver acceptance bandwidth.

$$dPRI = \frac{0.35 \cdot (2)^{0.5}}{0.8 \cdot B_v \cdot (SNR)^{0.5}} \quad (3-13)$$

$$dPW = \frac{0.7}{B_v [2 \cdot SNR]} 0.5 \quad (3-14)$$

The formulas above described are derived from the analysis done by Skolnik [Ref. 4] in chapter 11 of his book; but after comparing the obtainable standard deviation errors by using the formulas for frequency resolution, it was found that they gave very different values which need to be explained for application to an ESM receiver. These formulas apply to matched receiver superhets. Normally the measurement accuracy of a scanning (non-matched) superhet is its bandwidth. For example, a superhet tunable over a range (D) of one GHz. and having an acceptance bandwidth (Ba) of one MHz. would have a frequency resolution of 0.1% of its tuning range. If the tuning range were, for example two to four GHz.; then one could have a 0.1% accuracy with a bandwidth of two MHz.

For IFM receivers, especially the digital types, frequency resolution depends on the number of discriminators or the least significant bit (LSB) of the multi-discriminator, binary weighted, digital IFM.

Operational values for frequency accuracy in IFM receivers achieved by the author have been around 6 to 7 MHz and that is also mentioned as a standard frequency accuracy by C. L. Davies in his article [Ref. 14, p. 165-166] where he talks about frequency measurements. In general terms then,

the real accuracy should be, as stated initially, around 0.1 to 1% of the frequency value.

In wideband ESM receivers of the non-digital IFM type such as CVR or wide band superhets -such as microscan receivers- the noise bandwidth will be considerably less than the RF bandwidth. A good approximation for B_n is:

$$B_n = [2 \cdot B_{rf} \cdot B_v]^{0.5} \quad (3-16)$$

In any case, frequency resolution is a matter of bandwidth in tunable receivers. In IFMs it varies from very poor (equal to B_a in CVR) to good (0.1%) for digital IFMs.

The last parameter to be considered is the Angle of Arrival deviation, (ΔAOA). This is function of the kind of direction finding receiver used by the system, and for the purposes of this study it is assumed that this is an independent Receiver. Actually due to the wide ESM requirements in angle, power and frequency (and due to the platform physical limitations), an AOA accuracy of 5 to 7 degrees is considered to be typical and operationally reasonable [Ref. 14].

IV. ESM MEASURES OF EFFECTIVENESS

The tactical objectives imposed on an ESM System are to search for, intercept, locate and identify all the microwave emissions expected to be found in the probable theater of operations. If these are the requirements, a Measure of Effectiveness (MOE) must reflect quantitatively (and to a certain degree of accuracy), how well an ESM System is achieving these objectives.

The Probability of Intercept (POI) as defined by Ortiz and Giaquinto [Refs. 9 and 10] is a function of three independent factors: detectability, coincidence and identification. If reasonably good values are obtained for these three factors, the system should be accomplishing the tactical requirements, therefore POI appears to be a good ESM system measure of effectiveness. The model for the POI is in fact more realistic and complete than most of the definitions found in manufacturers brochures or EW texts. It emphasizes that all three conditions must be considered if a sensitive analysis is needed and it is intrinsically suitable as a decision tool. However, it is important to keep in mind that the interception problem will not be solved by just having a wide reception bandwidth, high sensitivity, and an omni antenna; it is necessary to quantify the relationships and

trade offs between them and then identify the improvable areas within the ESM receiver.

The nature of the variables involved in this problem are classified as controllable, uncontrollable (but predictable) and random. They will be identified as the model is developed with the fundamental purpose of highlighting their influence on the final output and how an ESM designer can overcome the induced handicaps by using his controllable parameters.

A. PROBABILITY OF DETECTION

The first independent factor considered in the POI model is the probability of detection. It is modeled by Skolnik [Ref. 4] and expanded for EW applications by Tsui [Ref. 3] where the ratio of IF bandwidth to video bandwidth produces a significant improvement, since the detector behaves as a filter. The probability of detection is a function of the signal power, receiver sensitivity, and the threshold level, although it is important to note that the ESM designer can obtain improvements in all three factors by devoting attention to the variables that are under his control.

The threshold level is obtained from:

$$Pfa = \exp \left[- \frac{V_t^2}{2 \Phi_0} \right] \quad (4-1)$$

where:

Φ_0 = Noise voltage variance

Pfa = Probability of False Alarm

Generally, the probability of false alarm (P_{fa}) is set to a reasonable value, and in this thesis it is set to 10^{-11} . Additionally, the noise variance is set to 1 [Ref. 3, p.22].

The probability of detection set of formulas according to Tsui [Ref. 3, Ch 2] is found in Appendices D and E of this thesis for Superhet and IFM receivers respectively.

It should be noted that Tsui has introduced the ratio of B_r to B_v in the probability of detection equations, therefore taking in to account what is called as the "processing gain" of the receiver. Many curves are shown in Tsui [Ref. 3, Ch 2] where the overall probability of detection improvement, due to the ratio B_r/B_v (Γ in the calculations), is emphasized. The available signal power at the receiver, and the receiver sensitivity, utilized in Tsui's equations were analyzed in Chapter 3 of this thesis.

B. PROBABILITY OF COINCIDENCE

The second independent factor of the POI is the probability of coincidence.

Before a detection can take place, the receiver must first obtain an alignment of different parametric windows. Self [Ref. 15] developed a simple but effective model that represents each parameter involved in the interception process as pulse train functions of time. Each window function is periodic, will have a window width (it will be of "squared" shape), and the phase or starting time is assumed to be

uniformly distributed. By using this model we can represent any of the periodic window function involved in the problem such as:

- Antenna rotation and beamwidth,
- Radar pulse repetition interval and pulse width,
- Superhet time to scan and time on frequency band,
- Mean hopping time and pulse width, etc.

In this thesis the above four mentioned window functions will be utilized for the analysis of the probability of coincidence.

Since the window functions are periodic pulse trains, their coincidences will also be periodic [Ref. 2, p.50] and will have the shape of a pulse train also. The coincidences pulse train will have a period given by:

$$T_o = \frac{\prod_{j=1}^n \left[\frac{T_j}{\tau_j} \right]}{\sum_{j=1}^n \left[\frac{1}{\tau_j} \right]} \quad (4-2)$$

where:

T_j = Period of the j th. window function

τ_j = Width of the j th. window pulse

Computational formulas derived from the above are found in Appendices H and I of this thesis for the desired windows.

The mean duration of the overlaps (τ_o) is given by:

$$\tau_o = \frac{1}{\sum_{j=1}^n \left[\frac{1}{\tau_j} \right]} \quad (4-3)$$

The probability of coincidence as function of time, $P_c(t)$ from Ref. 15 is expressed by:

$$P_c(t) = 1 - K \exp \left[\frac{-t}{T_o} \right] \quad (4-4)$$

where:

$$K = 1 - P_o \quad (4-5)$$

The average coincidence fraction P_o is given by:

$$P_o = \prod_{j=1}^n \frac{\tau_j}{T_j} \quad (4-6)$$

The required values for T_j and τ_j are defined as follows:

a) Antenna scan window: For the antenna scan window, T_j is the scan rate of the antenna in seconds (T_a), and τ_a is the time the 3 dB beamwidth takes to illuminate any target, say:

$$\tau_a = \theta_{3dB} / [360^\circ \cdot \text{Scan rate } (^\circ/\text{sec.})] \quad (4-7)$$

b.) Radar pulse train: The radar pulse train is by itself a window function defined by its period PRI and Pulse Width (PW).

c.) Superhet scan and time on frequency: The sweep period and acceptance bandwidth of a superhet receiver must be carefully chosen because they not only affect the probability of coincidence but also the noise level of the system. The time the receiver dwells on the frequency band of the emitter, τ_f , represents the window, and to ensure interception, this time must be greater than the pulse repetition interval.

Ortiz and Giaquinto [Refs. 9 and 10] have chosen τ_f to be 5 times the radar PRI for calculation purposes. The time on frequency is defined by:

$$\tau_f = \left[\frac{B_a + B_s/2}{D} \right] \cdot T_s = 5 \text{ PRI} \quad (4-8)$$

where for example:

B_a = 100 MHz; Receiver acceptance bandwidth

B_s = 250 KHz; Radar frequency spectrum app. 1/PW

D = 2 GHz; Sweep bandwidth of receiver

T_s = Scan time of receiver

From formula 4-7 we can calculate the values of:
 $T_s = 0.332 \text{ s.}$ and $\tau_f = 0.05 \text{ s.}$; which were used in the calculations of the Appendices.

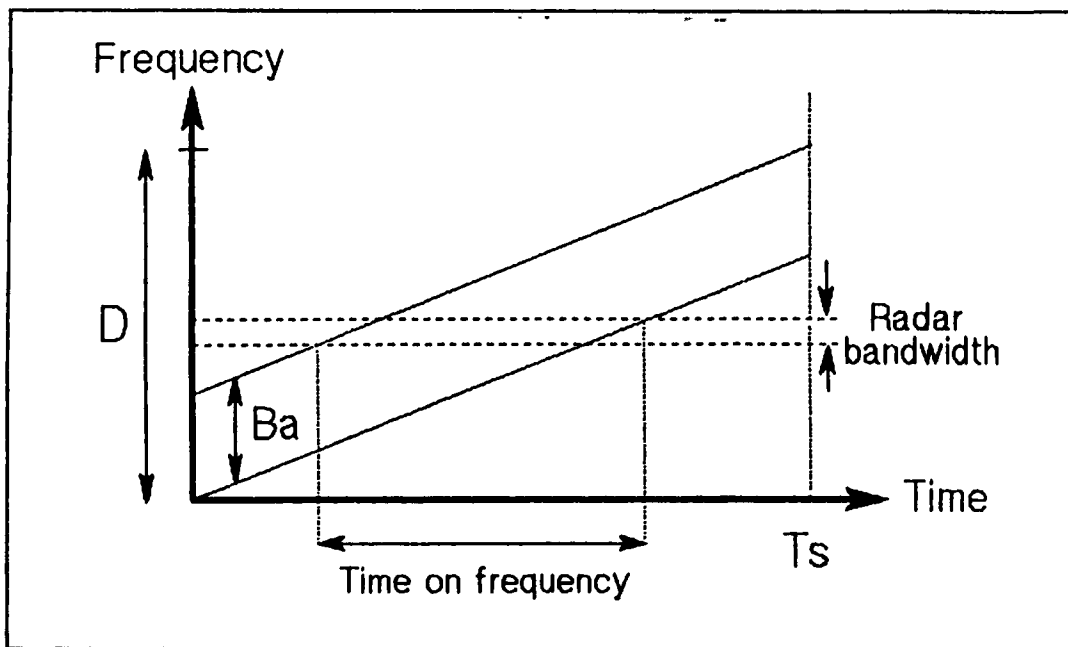


Fig. 9; Time to scan and time on frequency

The scan rate is also expressed as:

$$\frac{D}{T_s} = \frac{Ba}{\tau_f} \quad (4-9)$$

The shortest time on frequency τ_f is the minimum time required by the detector for energy buildup, and is inversely proportional to the acceptance bandwidth, $\tau_f (\text{min}) = 1/Ba$.

Therefore if this value is replaced in equation 4-19, we will be able to obtain the fastest scan rate achievable without loss of sensitivity [Ref. 3].

$$\frac{D}{T_s} = Ba^2 \quad (4-10)$$

$$B_a^2 = 10^{10} \text{ MHz/sec}$$

and actually our sweep rate is:

$$\frac{D}{T_s} = \frac{2 \text{ GHz}}{0.332 \text{ s.}} = 6000 \text{ MHz/sec.} \quad (4-11)$$

Which confirms that, for our example, we are scanning with a scan rate less than the maximum allowed.

d.) Mean hopping time and pulse width: The last window function of the model is derived from the fact that the radar is hopping over five different frequencies, therefore according to Self A. [Ref. 15] each frequency can be treated as an individual radar. If the frequencies are uniformly distributed, the period for a particular frequency to be repeated on the average is equal to five times the radar PRI, and since the time on frequency of the superhet receiver covers up to five times the PRI, it can intercept it. This problem must be considered also for an IFM receiver since for correlation purposes, the receiver needs to check the hopping period. The window width on the average will include two radar pulses since the receiver is dwelling for a time equal to five times the radar PRI, and as stated above, with this particular kind of hopping the

mean time for any particular frequency to appear again is five times the PRI.

C. PROBABILITY OF IDENTIFICATION

The identification of a radar emitter is done by comparing the received parameters with those stored in an internal library. Assuming that the stored parameters were accurately obtained and recorded, the probability of identification is a function of the quality of the receiver measurements, the number of parameters obtained, the characteristics of the processor and the electromagnetic density of the environment. Since in this thesis we are assuming a low intensity kind of encounter, we can assume that the processor will be able to handle appropriately all the information obtained by the receiver subsystem. The last assumption made the identification problem a direct function of the Receiver measurement accuracy/resolution, and the number of parameters measured.

From information theory we can state that in order to reduce uncertainty, any decision must be made over as many dimensions as there are available from the information source. This is particularly true in EW since it is required to sort classify and identify the signals intercepted; and all modern radar transmitters try to randomize their parameters in order to complicate the evaluation process at ESM reception.

Davies C. L. [Ref. 15, p.166] stated that the major parameters required for characterizing an emission are: angle of arrival, carrier frequency, pulse repetition interval (PRI) and pulse width (PW); and the availability and accuracy of them improves the identification capability of the System. From the parameters cited Angle of Arrival (AOA) is the most important since, while the other parameters may be varied by the transmitter, it is impossible to mask its AOA. The remaining parameters, arranged in order of importance, are frequency, PRI and PW.

The parameters availability can be modeled by using normally distributed accuracy formulas corrected to obtain realistic performance that is within 0.1 to 1% of the original parameter. Using one standard deviation ($\pm 1 \sigma$) as descriptor of variability gives a probability of occurrence of only 68.27 %. If we use two standard deviations ($\pm 2 \sigma$), then the probability of occurrence raises to 95.44% . Accuracy and resolution are two closely related terms. Resolution is the finest resolving power of the system that will allow for differentiation of two signals closely spaced in the parameter spectrum. On the other hand, accuracy of the measurements depends on many factors but its minimum value is defined by the resolution of the system. It is important to state that a system cannot measure more accurately than its resolving capability, but signal variations that produce

inaccuracies may well affect a parameter measurement if they are significant; that is bigger than the resolution cell.

For the case of frequency measurements, the superhet and IFM resolution problems are different. In the first case, the resolution is defined by the IF bandwidth of the system, while in most modern IFM systems it is given by the least significant bit of the digital parameter word.

For the model of this thesis, is assumed an 10 bit frequency word in the IFM system which makes the frequency resolution to be approximately 2 MHz. out of a 2 GHz. frequency band.

The accuracy measurement formulas derived from chapter three of this work and corrected for general EW application are as follows:

$$\sigma_F = \left[\frac{3}{\pi^2 \cdot PW^3 \cdot B_n \cdot SNR} \right]^{0.5} \quad (4-12)$$

Frequency identification occurs with a high probability if $(4 \cdot \sigma_F) / f_c$ is < 0.001 ; and if the frequency resolution is also within that limit (0.001 of the original frequency).

$$\sigma_{PRI} = \frac{0.35 \cdot 2}{0.8 B_v \cdot SNR^{.5}} \quad (4-13)$$

PRI identification occurs if $(4 \cdot \sigma_{PRI}) / PRI < 0.01$

$$\sigma_{PW} = \frac{.7}{B_v \cdot SNR^{.5}} \quad (4-14)$$

PW identification occurs if $(4 \cdot \sigma_{PW})/PW < 0.01$

The probability of identification can be modeled from combinatorial analysis and using the utility factors approach recommended by Glenn [Ref. 7]. Therefore we will be able to weight properly each of the possible combinations of the parameters at reception according to the importance of each of them and make use of MATHCAD's MAX function to select the most valuable combination. The utility factors of the parameters at reception are:

- Angle of arrival w1 = 0.3
- Carrier frequency w2 = 0.28
- Pulse repetition interval w3 = 0.25
- Pulse width w4 = 0.19

A sensitivity analysis was applied to these utility factors in order to check their influence in the identification process. This will be discussed in the next chapter during the analysis of the output.

When a parameter is measured, and its deviation is within the required limits, then we will be able to use it.

This is modeled by using MATHCAD's Heaviside's step function:

$$d(x) = \Phi (\text{limit} - (4\sigma/\mu)) \quad (4-15)$$

Therefore if the ratio, deviation/mean, is less than the required limit a "1" is returned, otherwise it will return a "0". Finally, with the use of combinatorial analysis, an identification array is modeled that includes all the available parameter combinations at reception that may identify a certain transmitter, weighting each particular combination according to which parameters it is composed of, and using the standard deviation model to determine which parameters were available at every measurement. In this way, the combinations are arranged from top to bottom with the most valuable at the top and the least at the bottom. The weighting factor used in every row (combination), was chosen to be the square root of the summation of the weights of the respective parameters involved. The usage of this array guaranteed that only the row which included all the available measurements will be selected, avoiding redundant choices. This is true because, for example, if three parameters are identified, all combinations will acquire a certain value but only the one which includes all three must have been selected. Initially the weighting factors were defined just by the sum of the weights of the respective deviations within each

combination; but this approach was discovered to overweigh the combinations which had more elements (or more weight). Therefore when only two or three parameters were identified the probability of identification was decided not by the combination which contained the identified parameters but by the more valuable combination (the one which includes measurements of all the parameters) even though it did not have all the deviations identified. This was because the weights overcame the lack of parameters. It is clear then that the model was not correct, since even though it included all the variables of the problem, it always selected the same combination (the one with the highest weighting factor).

$$\begin{aligned}
 (w_1+w_2+w_3+w_4)^5 &= 0.25 (dAOA+dF+dPRI+dPW) \\
 (w_1+w_2+w_3)^5 &= 0.333 (dAOA+dF+dPRI) \\
 (w_1+w_2+w_4)^5 &= 0.333 (dAOA+dF+dPW) \\
 (w_1+w_3+w_4)^5 &= 0.333 (dAOA+dPRI+dPW) \\
 (w_2+w_3+w_4)^5 &= 0.333 (dF+dPRI+dPW) \\
 (w_1+w_2)^5 &= 0.5 (dAOA+dF) \\
 (w_1+w_3)^5 &= 0.5 (dAOA+dPRI) \\
 (w_1+w_4)^5 &= 0.5 (dAOA+dPW) \\
 (w_2+w_3)^5 &= 0.5 (dF+dPRI) \\
 (w_2+w_4)^5 &= 0.5 (dF+dPW) \\
 (w_3+w_4)^5 &= 0.5 (dPRI+dPW) \\
 (w_2)^5 &= dF \\
 (w_3)^5 &= dPRI \\
 (w_4)^5 &= dPW
 \end{aligned}
 \tag{4-16}$$

The weight differences from row to row were also too significant. As a result, weight difference became the key in the selection process even though in some cases there was a lack of other information.

In order to solve this problem, the differences between the rows of the array created in the original model were reduced by taking their square root. Then by using MATHCAD's MAX function, we were able to choose the combination which had the highest value in the probability of identification array.

The following example illustrates the weighting factors problem. Suppose that the system has identified frequency, PRI, and PW, and MATHCAD'S MAX function is used. Then:

$$dAOA = 0; \quad dF = 1; \quad dPRI = 1; \quad dPW = 1$$

a) Method No. 1: Weight = Sum of weights

$$\begin{aligned} 1.0 \quad (0.25) \quad (dAOA+dF+dPRI+dPW) &= .75 \quad . \quad \text{wrong selection} \\ 0.9 \quad (0.33) \quad (dAOA+dF+dPRI) &= .594 \\ 0.7 \quad (0.33) \quad (dAOA+dPRI+dPW) &= .462 \\ 0.6 \quad (0.33) \quad (dF+dPRI+dPW) &= 0.6 \end{aligned}$$

b) Method No.2: Weight = (Sum of weights)^{.5}

$$\begin{aligned} 1.0 \quad (0.25) \quad (dAOA+dF+dPRI+dPW) &= .75 \\ 0.948 \quad (0.33) \quad (dAOA+dF+dPRI) &= .626 \\ 0.837 \quad (0.33) \quad (dAOA+dPRI+dPW) &= .557 \\ 0.774 \quad (0.33) \quad (dF+dPRI+dPW) &= .774 \quad . \quad \text{right selection} \end{aligned}$$

Therefore by using MATHCAD's MAX function in method No.2 the correct selection was made.

Parameters Measured				PROBABILITY OF IDENTIFICATION P(id)
AOA	FREQ	PRI	PW	
X	X	X	X	1.00
X	X	X		0.911
X	X		X	0.877
X		X	X	0.86
	X	X	X	0.85
X	X			0.761
X		X		0.741
X			X	.7
	X	X		0.728
	X		X	0.685
		X	X	0.663
	X			0.529
		X		0.5
			X	0.436

Table 1; Probability of Identification based on combinatorial analysis, weighting factors, and parameter accuracies.

The combination that matched the parameters identified was weighted the most valuable compared with the other possible combinations within the array.

The angle of arrival identification was particularly difficult to model because it depends on the direction finding (DF) receiver system employed. Consequently, in order to solve it we established an AOA rms. error of 4 degrees as a reference and -50 dBm as its sensitivity level. These are typical values of performance by equipment used for tactical purposes. Generally, most ESM systems have a separate DF receiving system that is interfaced with the radio frequency system. The most common DF system uses amplitude comparison techniques and its receivers are broadband crystal video in an omni-directional array of 4, 6 or 8 antennas.

The DF accuracy obtained in the model will be a function then of the strength of the signal at reception, the sensitivity level, and the ratio between the actual angular error of the system compared with the stated reference. The actual rms error was set to 5 degrees.

As documented in this chapter, the POI is a function of three independent factors, probability of detection, probability of coincidence, and probability of identification. Each one of these factors being particularly defined, the measure of effectiveness reflects the complex interaction of the many inputs involved, and allows the designer to selectively analyze the parameters influence in the overall performance variation.

V. ANALYSIS

In the analysis section of this thesis we will go over the outputs of the different MATHCAD files which were developed in order to represent the POI as explained in chapter four. The causes and effects related to each particular set of curves will be discussed. The generated curves are:

- Main lobe and side lobes probability of detection
- Main lobe and side lobes probability of coincidence
- Main lobe and side lobes probability of identification
- Main lobe and side lobes probability of intercept

The curves were modeled from both IFM and superhet receiver special characteristics, as defined in appendices B and C. The aircraft was initially placed at 4000 m. height, (279 Km. maximum range) on the ESM horizon line (tangential to the Earth), beyond the estimated radar maximum range, which will allow us to observe typical performances.

A. PROBABILITY OF DETECTION ANALYSIS

The analysis starts with the probability of detection curves Figures 9, 10 and 11. Figure 9 shows the probability

of detection of the radar's sidelobes as a function of time for a superhet receiver. Each time unit represents 200 seconds of flight. Therefore after flying 800 sec. (app. at 200 Km. from the target), this receiver will act as an omnidirectional antenna by receiving the radar all the time. It should be noted that the probability of detection for the radar main lobe, as expected, was always unity across the time window of interest. The equations used from Tsui [Ref. 3, Ch. 2], which include the processing gain effect due to the ratio B_r/B_v , actually reduce the SNR required at the receiver to obtain a certain probability of detection given a probability of false alarm. In fact, the required SNR to produce a 0.999 probability of detection is approximately 10 dB., when the $P_{fa} = 10^{-11}$; that might seem too small.

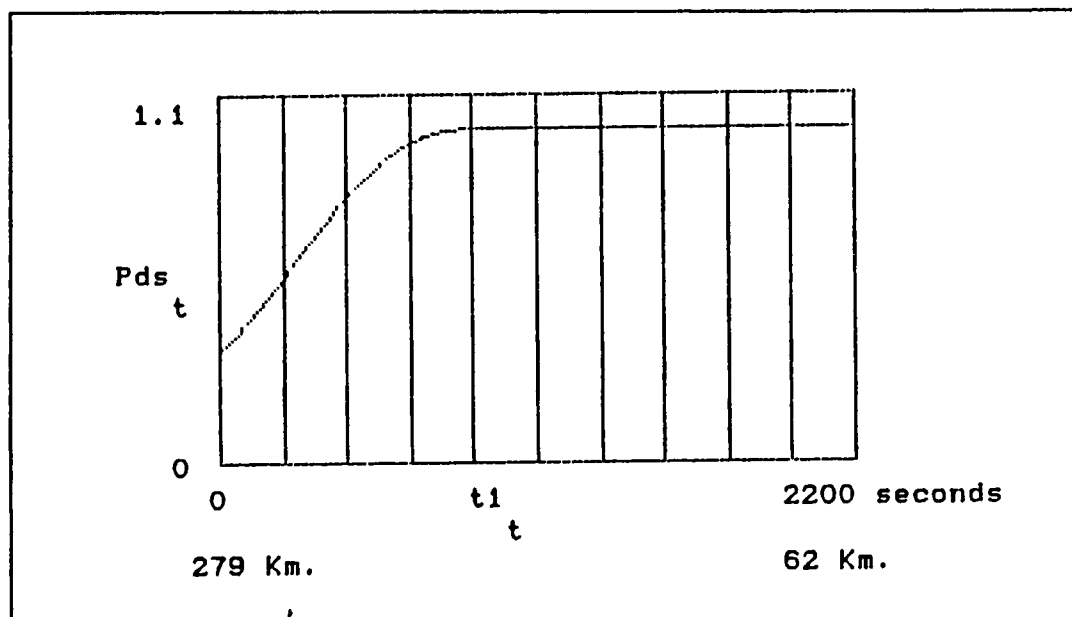


Fig. 9 Radar side lobes probability of detection vs. time superhet receiver case.

The probability of detection versus time, for the example IFM receiver, showed that: due to the rms. noise power increase (wider bandwidth), this receiver was unable to detect the radar sidelobes during all the flight time. Near the end of the time line (62 Km. from target) the SNR for the radar side lobes was just 0.88 dB; too low for achieving detection, and this agrees with the curves from Tsui [Ref. 3, Ch. 2]. In any case, as Figure 11 shows, it did detect the radar mainlobe with a probability of one along the trajectory.

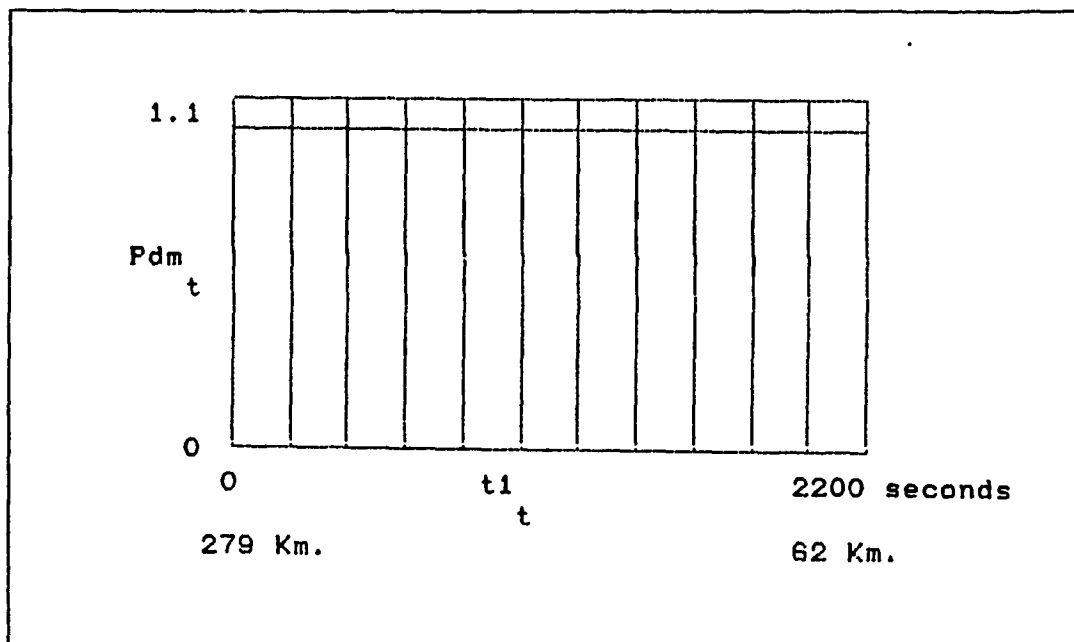


Fig. 10 Radar main lobe probability of detection vs. time; superhet receiver case.

The analysis of the probability of detection factors showed that the superhet receiver had the advantage of having detection of both the radar main and side lobes. On the other

hand the IFM receiver was able to detect the radar emission only when the radar main lobe pointed at it.

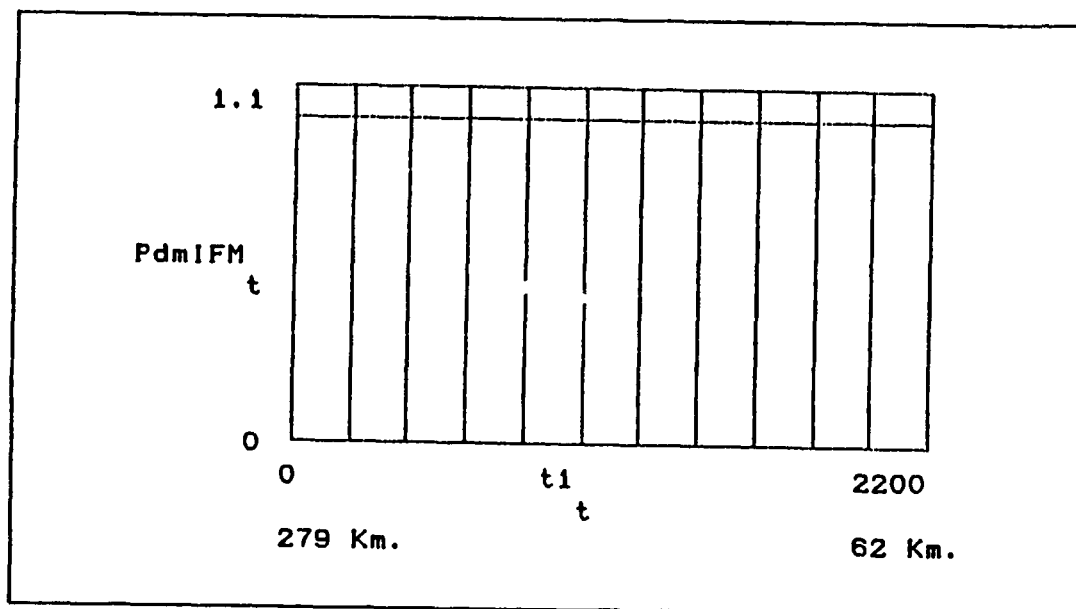


Fig. 11 Radar main lobe probability of detection vs. time; IFM receiver case.

B. PROBABILITY OF COINCIDENCE ANALYSIS

The probability of coincidence vs. time in the superhet receiver was very low as can be observed in Figure 12, where after 2200 seconds of flight the probability of coincidence is 0.06. This is the disadvantage of using a narrowband scanning receiver against a frequency hopping radar.

From the respective MATHCAD file, the average time between coincidences (period) from a superhet receiver for the mainlobe and sidelobes was found to be 8 h. 50 min. 30 sec., and 3 min. 42 sec. respectively (1om and 1os in Appendix H).

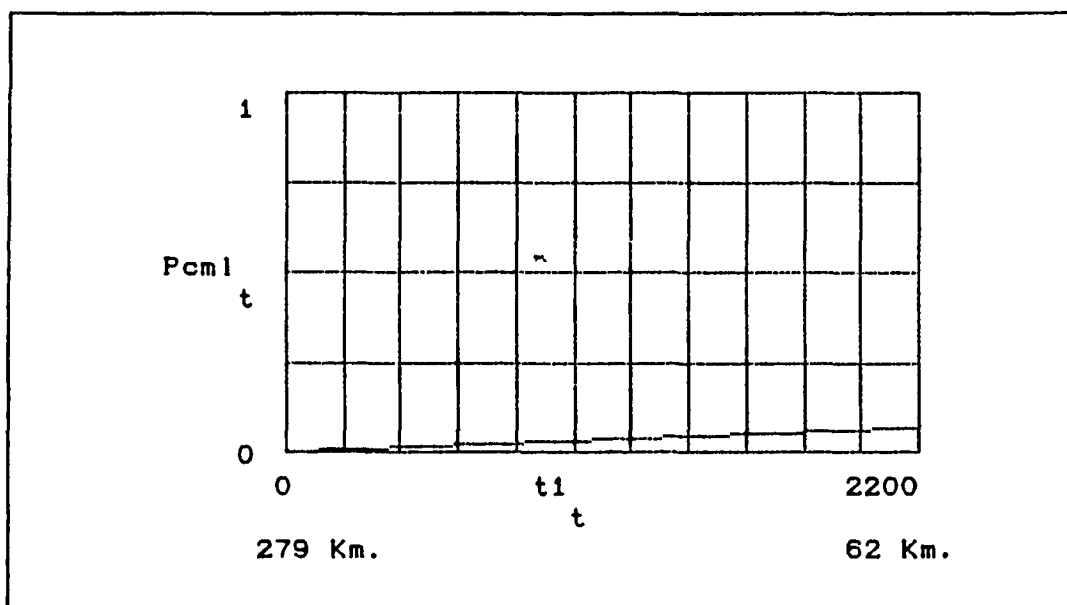


Fig. 12 Superhet receiver main lobe probability of coincidence versus time.

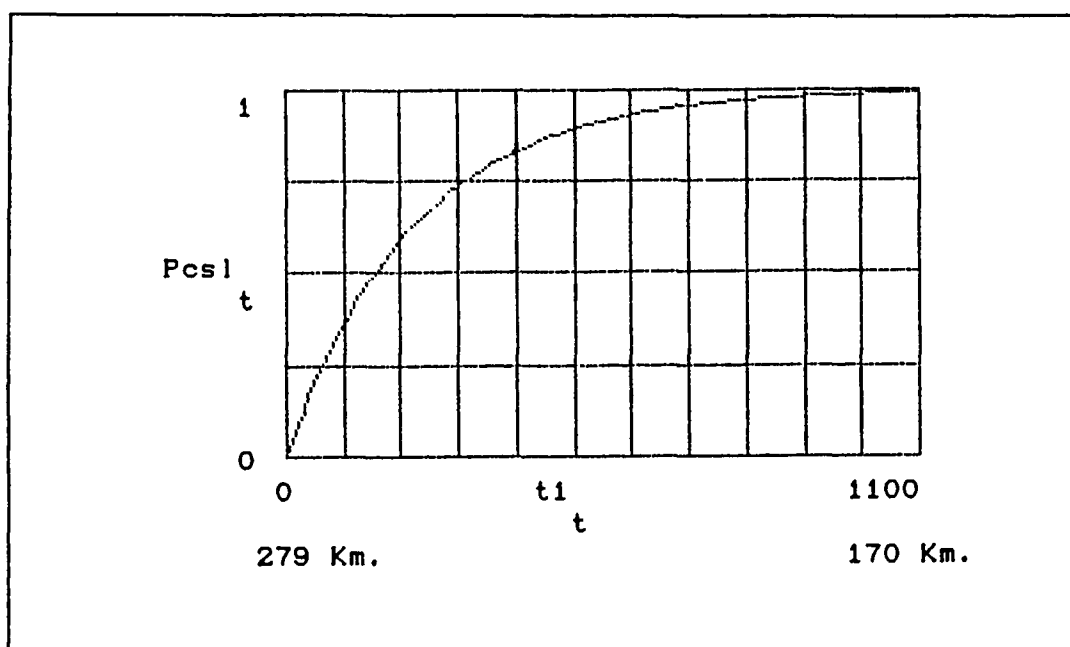


Fig. 13 Superhet receiver side lobes probability of coincidence versus time.

The low performance induced by increasing the number of window functions is drastic, which explains why modern radar designs are trying to randomize (within limits) most of the transmitted parameters.

One way to improve the probability of coincidence is by elimination of one window function or optimization of the window functions that are under our control; the first solution is possible if IFM receivers are used. IFM receivers can observe instantaneously, wider bandwidths eliminating the receiver-scan window function (setting it equal to one). This effect is shown in Figures 14 and 15, for main and side lobes probability of coincidence, respectively.

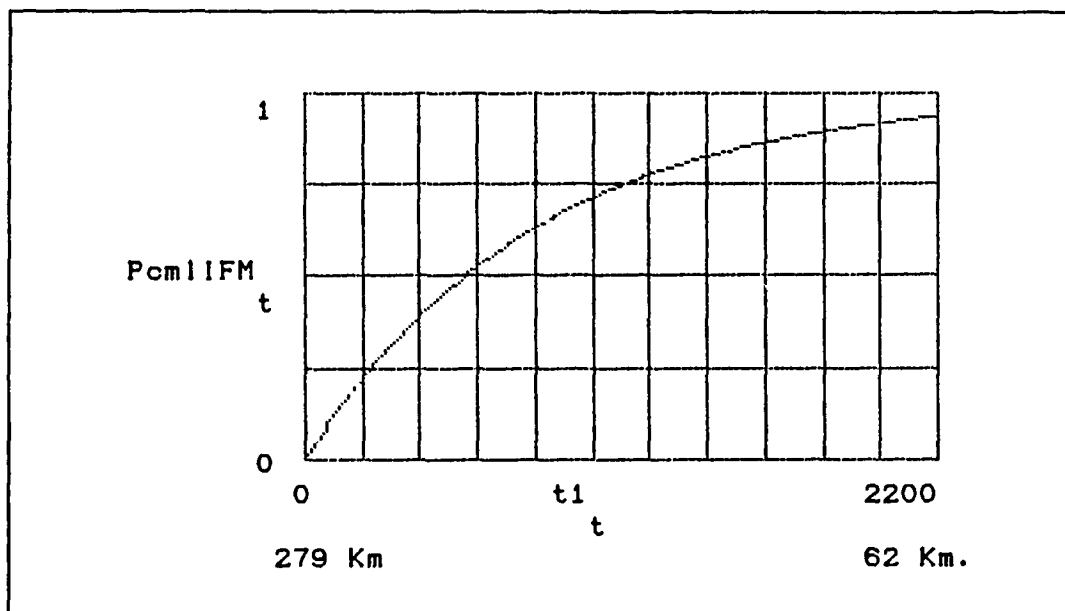


Fig. 14 IFM receiver main lobe probability of coincidence versus time.

In Figure 15 a 0.9 probability of coincidence (mainlobe) at the end of the time window of interest is achieved; and in Figure 16 it can be seen that the probability of coincidence approaches unity very fast, which is a tremendous improvement compared with the superhet case.

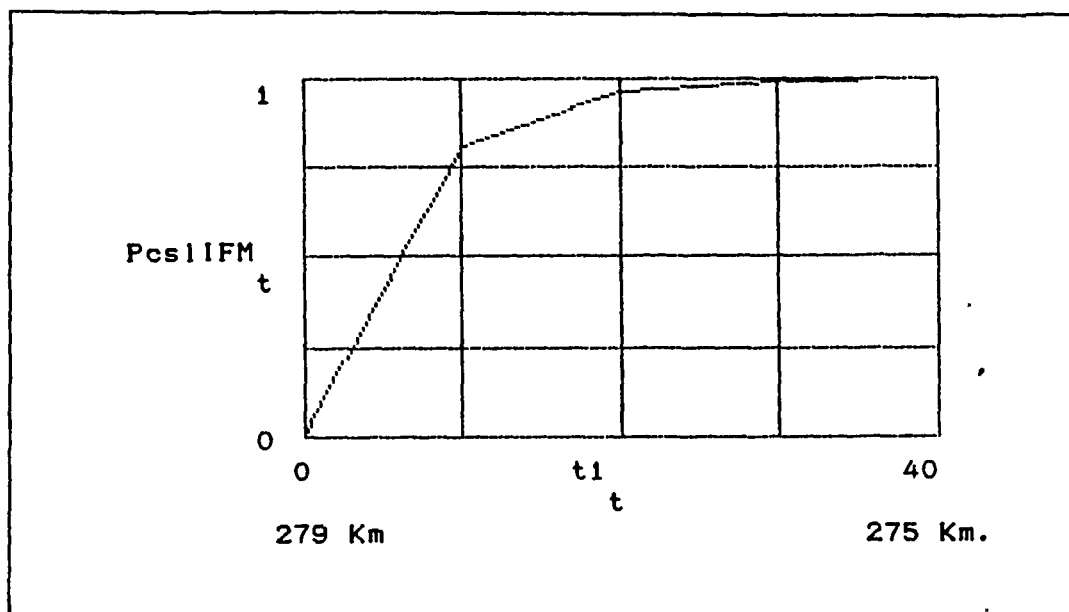


Fig. 15 IFM receiver side lobes probability of coincidence versus time.

In general it can be said that the probability of coincidence curves gave the IFM receiver a significant performance advantage when compared with the superhet receiver performance against both the radar main and side lobes.

C. PROBABILITY OF IDENTIFICATION ANALYSIS

The probability of identification is quite empirical since, even though the accuracy of the measurements relates to identification of parameters, these formulas were evaluated with assumed errors which try to mimic realistic ESM scenarios.

For the case of superhet receiver, it can be observed in Figure 16 that for main lobe reception, the probability of identification has a value of 0.78 during all the time of interest. This is explained because the model is identifying all the parameters except frequency (wider resolution). Additionally AOA, which was set to be the ratio of a reference value to the actual accuracy, had an accuracy of 0.8 ($4 / 5 = 0.8$); therefore, the identification array chose the fourth combination giving us a probability of identification of 0.79.

For the superhet side lobes case, the probability of identification has a value of 0.48 from $t = 0$ s. to 1450 s. where it jumps to 0.663. The first value is due to PRI measurement alone, and after closing in range for 1450 s. the system is able to identify additionally the emitter PW, thus improving its identification contribution.

For an IFM receiver, the mainlobe identification problem is depicted in Figure 17, where (at $t = 1320$ s.) the probability of identification jumps from 0.84 to 0.95. This jump is due to PW accuracy improvement at that particular

time, providing thereafter all the parameters needed for identification purposes.

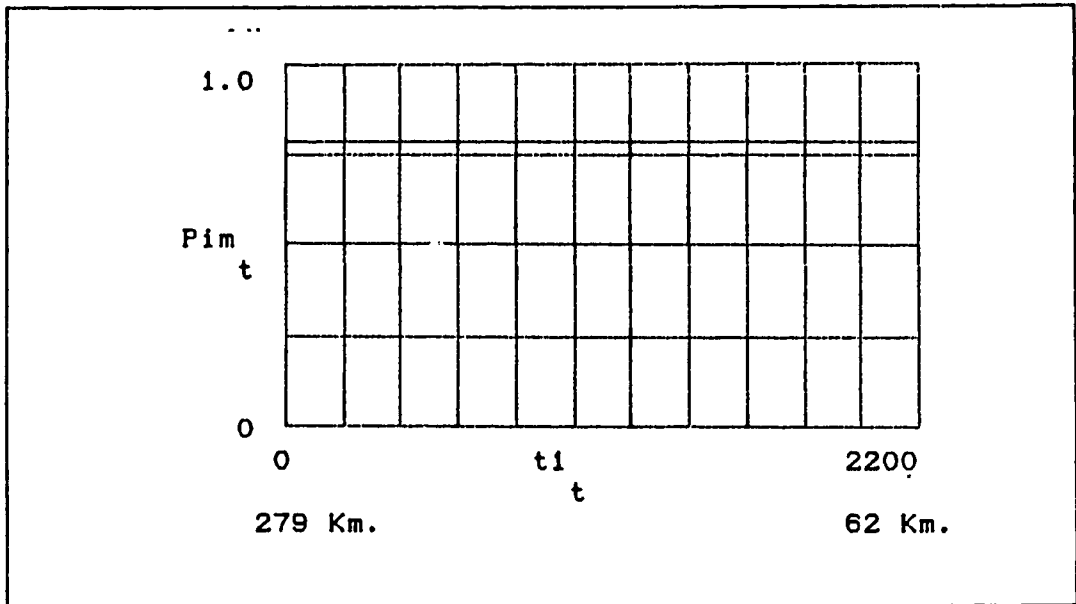


Fig. 16 Superhet receiver main lobe probability of identification versus time.

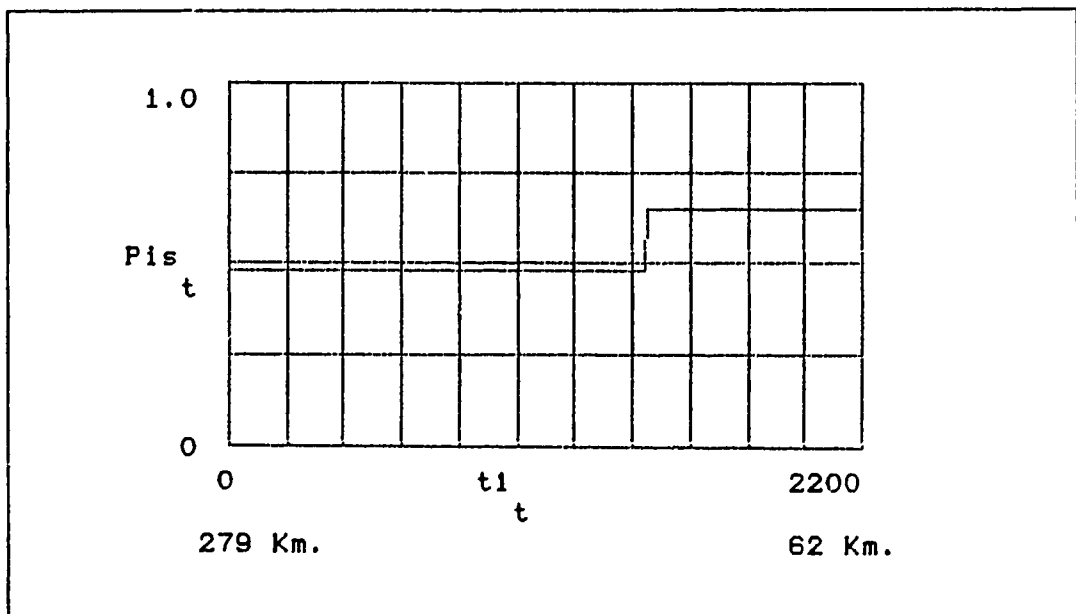


Fig. 17 Superhet receiver sidelobes probability of identification versus time.

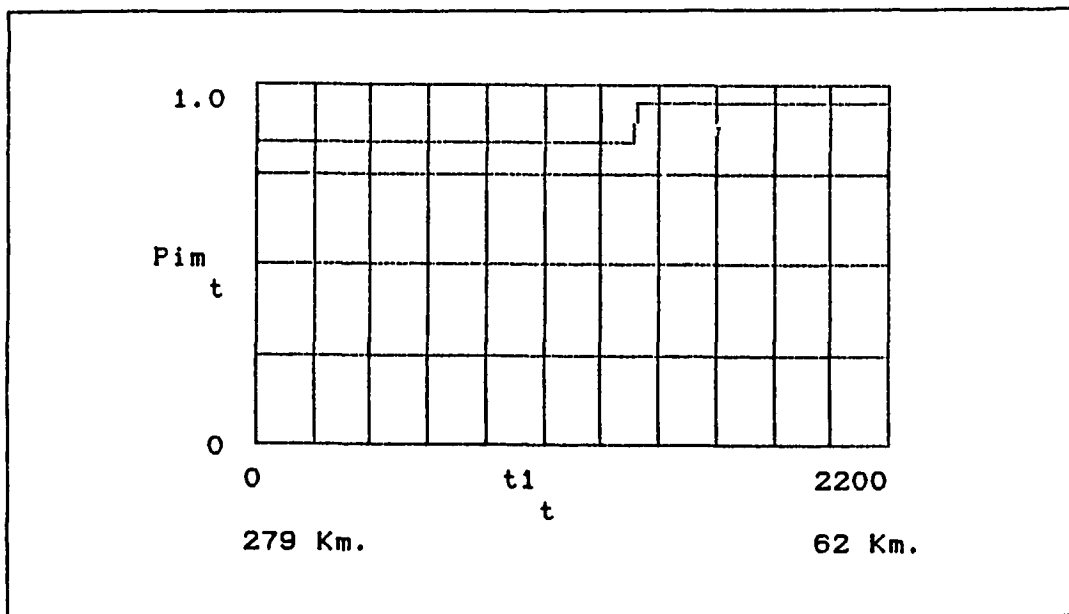


Fig. 18 IFM Main lobe probability of identification vs. time

Figure 19 plots the side lobes case of the same problem. In here we find a straight line, representing a constant probability of Identification value of 0.728. This value comes from having achieved only PRI and frequency accuracy, no other parameter was available during the time window.

The probability of identification plots have shown an considerable advantage of the IFM on main and side lobes emitter identification. The main source of this difference is due to the frequency identification capability of the IFM receiver (fine frequency resolution). Frequency availability has been weighted as one of the most valuable parameters for identification purposes.

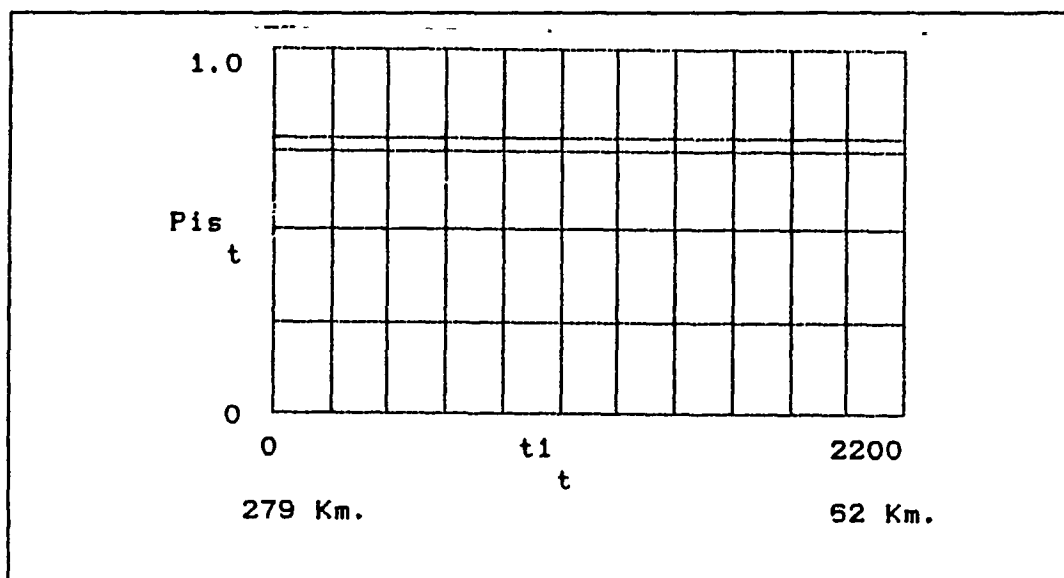


Fig. 19 IFM side lobes prob. of identification vs. time.

D. POI ANALYSIS

Finally all the above probabilities are used to model the overall probability of intercept (POI), this may be expressed as A function of two mutually exclusive events:

$$POI = POIml + POIsI - (POIml \cdot POIsI) \quad (5-1)$$

where:

POIml = Probability of intercept main lobe

POIsI = Probability of intercept side lobes

Each one of the above variables are derived from three mutually independent events:

$$POIm1 = PDm1 PIDm1 PCm1 \quad (5-2)$$

$$POIs1 = PDs1 PIDs1 PCs1 \quad (5-3)$$

where:

PDm1 = Probability of detection - main lobe -

PDs1 = Probability of detection - side lobes -

PIDm1 = Probability of identification - main lobe -

PIDs1 = Probability of identification - side lobes -

PCm1 = Probability of coincidence - main lobe -

PCs1 = Probability of coincidence - side lobes -

The above data was generated for every time step within each of MATHCAD file. The outputs were also stored in the form of files in such a way that the POI file recovered the component files, did the calculations above explained, and outputed the POI results. The plot shown in Figure 19 represents the overall probability of intercept for both IFM and superhet receivers in this particular scenario.

The most significant aspect about Figure 20 is that the IFM performance did not make use of any Side lobe interception since it was never able to detect it. In addition, the performance of the superhet receiver was not as good as that of the IFM even though it achieved very good detection (SNR) and identification (theoretical from SNR) of main and side lobes along the time line. From this we can deduce that the probability of coincidence is the most significant factor

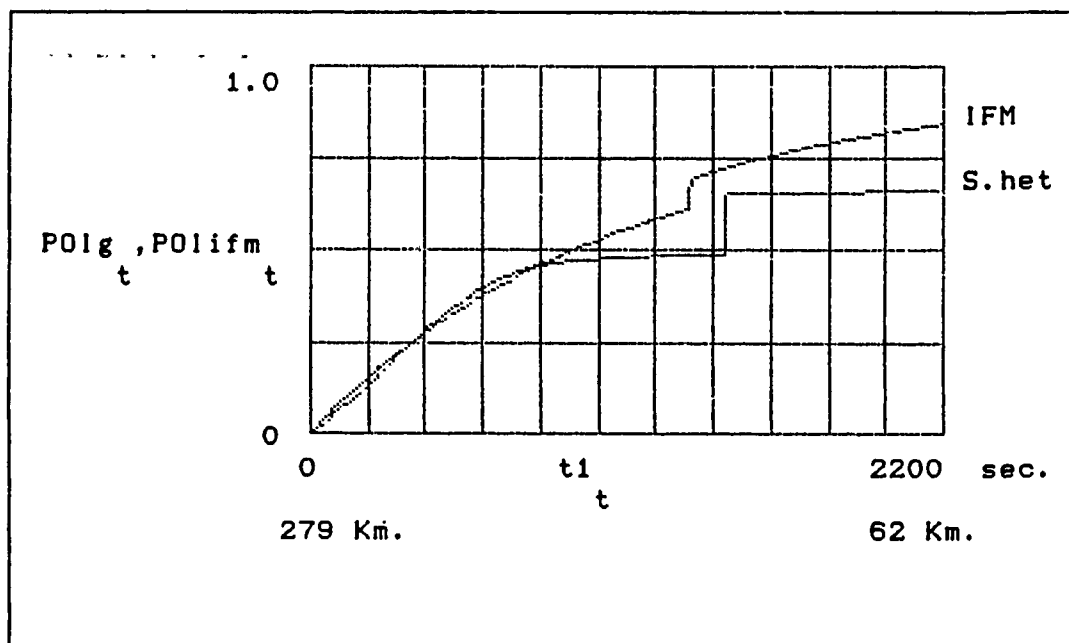


Fig. 20 Probability of intercept versus time, superhet and IFM receivers performance.

in these scenarios and, as has been discussed in many publications, it represents a key point for superhet receivers which suffer the larger degradation in their interception capabilities. In order to investigate this further, it was decided to test the model against the same radar but while transmitting a constant carrier frequency. The probability of intercept plot obtained is in Figure 21.

This confirms the influence of the probability of coincidence in the general performance. By fixing the carrier frequency, one eliminates one of the window functions, thereby improving both systems in an equal manner. Now the superhet

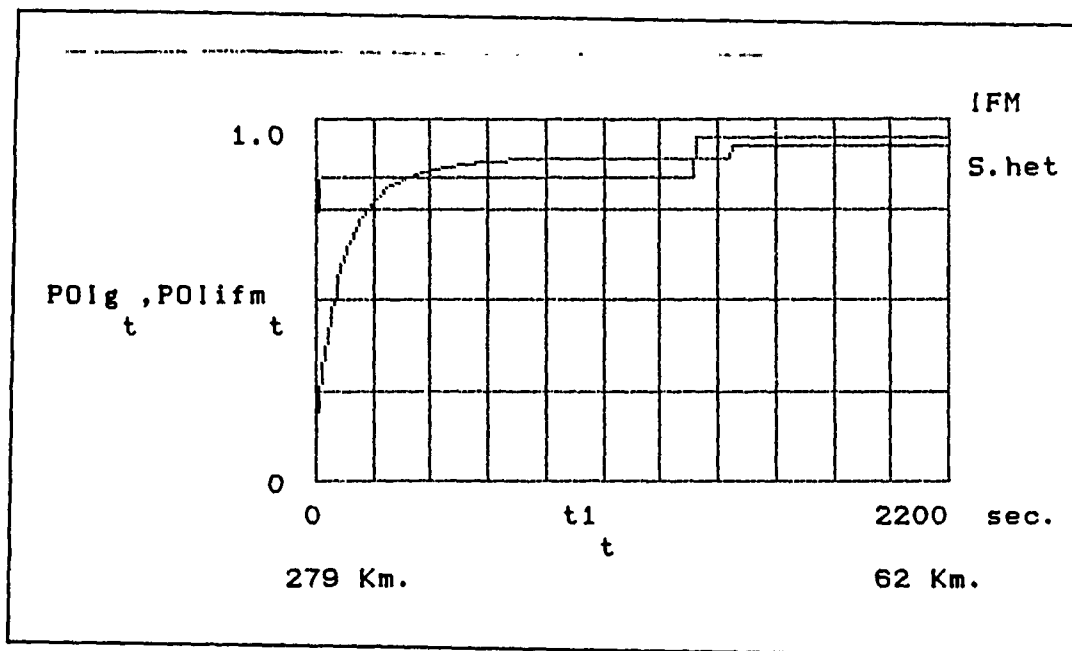


Fig. 21 Probability of intercept vs. time, superhet and IFM performances against a fixed frequency radar.

receiver performs better until app. $t = 1300$ s. because the additional weighting of having both main and side lobes interception supplies a significant increase in POI. This overcomes the additional window function that the Superhet was encountering (scanning in frequency).

Both curves show a "jump" approximately between $t = 1300$ and 1450 s. This is derived from the PW identification, as explained above.

In general terms, when dealing against a fixed frequency radar, the superhet receiver experiments a considerable improvement. This improvement is basically due to better probability of coincidence performance, and if frequency

resolution is refined by the use of a narrower band, better identification values can be obtained.

E. SENSITIVE ANALYSIS OF WEIGHTING FACTORS

Finally, the weighting factors were tested in order to check their influence in the probability of identification and in the probability of intercept. The weighting factors as summarized in Table 2. show the use of the following weights:

Figure 21 Weight set a.	Figure 22 Weight set b.	Figure 23 Weight set c.
dAOA = 0.4	0.35	0.35
dF = 0.3	0.35	0.3
dPRI = 0.2	0.25	0.2
dPW = 0.1	0.05	0.15

Table 2. Weighting factors sets.

As can be seen in Figure 21, the use of the first set of weights does not affect the initial probability of intercept (Figure 19) except by a small reduction in the superhet receiver. The performance is otherwise nearly the same as for Figure 20. Reviewing the probability of identification plots it was found that the side lobes jump at $t = 1450$ s. changed initially from 0.479 to 0.648 (Figure 16) but in Figure 21 they changed from 0.447 to 0.557. For the IFM case the variations were not significant.

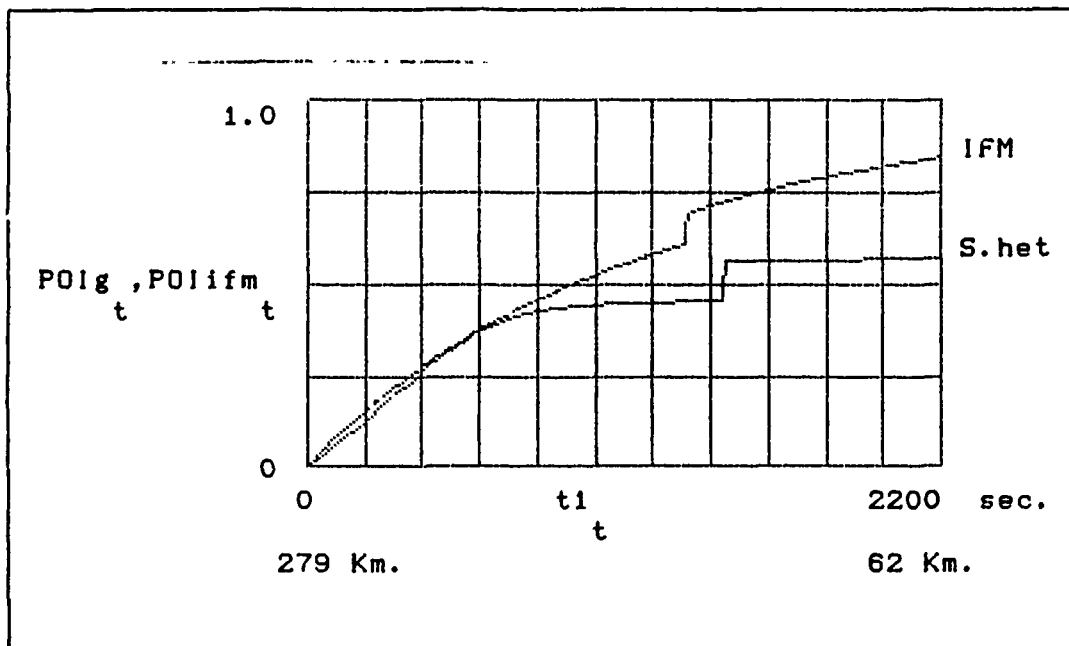


Fig. 22 Superhet and IFM performances; $dAOA = 0.4$, $dF = 0.3$, $dPRI = 0.2$, and $dPW = 0.1$

Following the a-set weights evaluation, b-set weights were substituted and the plot of Figure 22 was obtained. It can be noted a significant decrease in the probability of intercept curves, and especially in the superhet curves, as compared with Figure 20; but if they are compared with Figure 22 it can be found after the jump both Figures show no difference. One observes an approximate 0.2 improvement, in the superhet receiver, before the jump takes place. With the last weights set, Figure 23 is obtained; which is very similar to Figure 22.

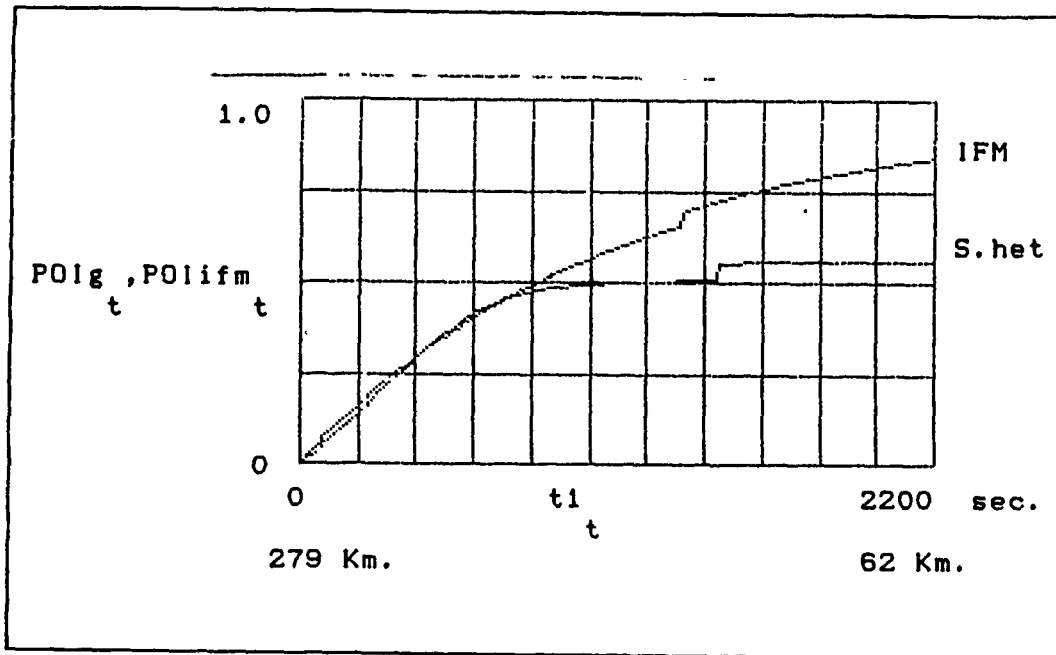


Fig. 23 Superhet and IFM performances; $dAOA = 0.35$,
 $dF = 0.35$, $dPRI = 0.25$, $dPW = 0.05$

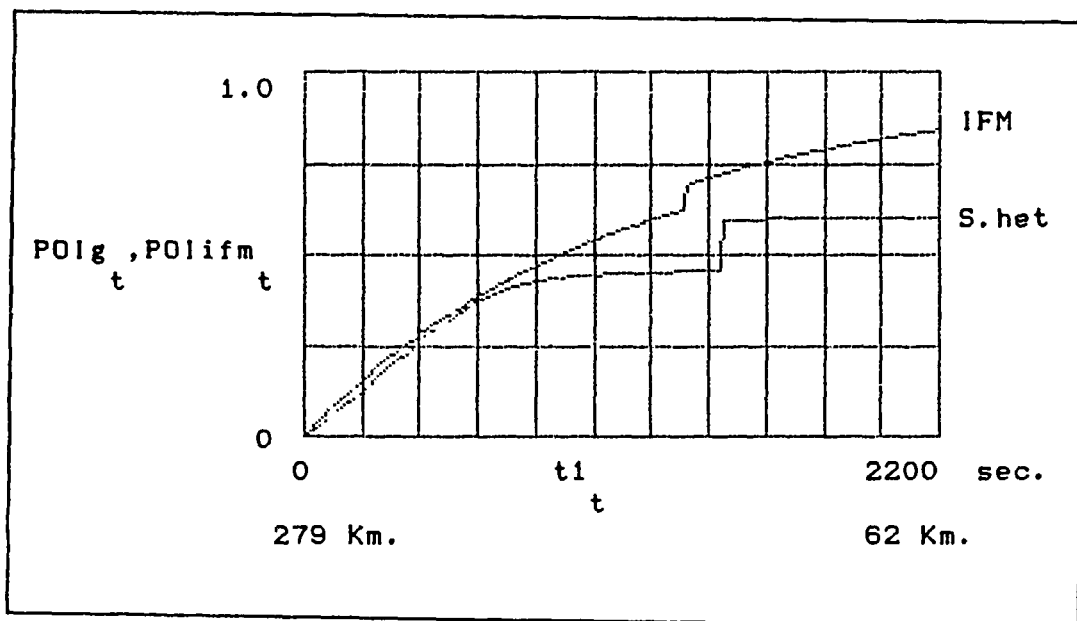


Fig. 24 Superhet and IFM performances; $dAOA = 0.35$, $dF = 0.3$,
 $dPRI = 0.2$, $dPW = 0.15$.

The only difference is that the jump in the superhet POI is larger with set c. This is because PW is now weighted more heavily.

The precedence used in this work for the parameters weighting should be kept unless extremely good processor performances would allow the use of higher utility factors consequently modifying the established precedence. It would be desirable also to test operationally for the values of each parameter with special consideration of the processor capabilities.

As can be observed in the plots, the shape of the POI curves would not be altered but their time to achieve a POI value could be reduced with variations in the weighting factors. In any case, the approach used in this thesis is useful since it allows good approximate results.

VI. CONCLUSIONS

A. GENERAL CONCLUSIONS

1) During ESM systems performance evaluation many variables and complex trade offs between them must be considered. The model used in this work is robust and expands the qualitative evaluations commonly done with a "good", "fair", or "poor" grading policy.

2) Within the scope and scenarios of this thesis it can be concluded from the measure of effectiveness, that the IFM receiver had a better performance than the Superhet.

3) When dealing with frequency agile radars, the fact of having a very sensitive receiver by itself does not solve the interception problem, as indicated by the Superhet receiver curve. The ESM designer must work within the coincidence problem to improve the probability of coincidence, modifying the windows under his control. Rotating antennas are not appropriate for tactical purposes since their use will imply an extra window function in the coincidence problem.

B. SPECIFIC CONCLUSIONS

1) The performance observed in the superhet receiver against a fixed frequency transmitter was superior to the IFM receiver in its capability of detecting the sidelobes. It is

well known that superhet receivers are capable of achieving also higher frequency accuracy as compared with IFM receivers.

2) The probability of coincidence requirement for a tactical ESM system must be always considered.

3) Sensitivity still remains a very important parameter since signal value is critical at every step in the calculations.

C. OPERATIONAL CONCLUSIONS

1) In peace time, when threat radars are more indiscrete, a superhet receiver is the optimum choice.

2) In wartime tactical operations, the IFM is superior because of its shorter time to interception even though its accuracies are not as high. For initial tactical success, the ESM operator must utilize his assets to the maximum continuous extent possible.

3) During tactical surveillance operations the aircraft should always fly below the line of sight of the emitter which is tangential to the earth's surface and away from the tangential point. This is the worst detection region for the radar, and if the aircraft is flying high enough, the ESM range becomes the best weapon at hand. As the ESM aircraft does its approach towards the emitter, it must lower its altitude continuously in order to stay in the radar diffractive zone. ESM ranges obtainable with sensitivities

of -65 dBm. or better are considerably greater than the maximum radar detection range.

VII. RECOMENDATIONS

1) Operational test should be conducted to compare and validate the data presented here. The combinatorial-weighting factors approach presented appeared to give artificially high accuracy values.

2) During peace time operations; ESM aircraft crews should concentrate their efforts toward fine tuning radar signals in order to upgrade current threat libraries.

APPENDIX A: SENSITIVITY REQUIREMENTS

SENSITIVITY REQUIREMENTS FOR AN ESM RECEIVER =====

The required sensitivity is a function of the enemy radar and of the operational requirements imposed such as detection range or pulse density.

Enemy radar parameters:

$P_t := 250 \cdot 10^3$	watts	Peak power
$G_t := 1585$		Antenna Gain (app. 32 db)
$\tau := 4 \cdot 10^{-6}$	s	Pulse width
$\lambda := 0.1$	m	Wavelength (in meters) S band radar
$L_t := 2$		Transmitter losses
$g := 1$		Multipath coefficient
$h_t := 20$		Radar antenna height (m)

ESM parameters:

$G_{esm} := 1$		Omnidirectional Antenna
$\alpha := 20$		Aircraft's R. C. S.
$L_{esm} := 2$		ESM receiver losses
$h_{esm} := 1000$		ESM aircraft height (m)

1.- ESM AND RADAR SENSITIVITY REQUIREMENTS AS FUNCTION OF RANGE

R := 1,5 ..1000

Range variations

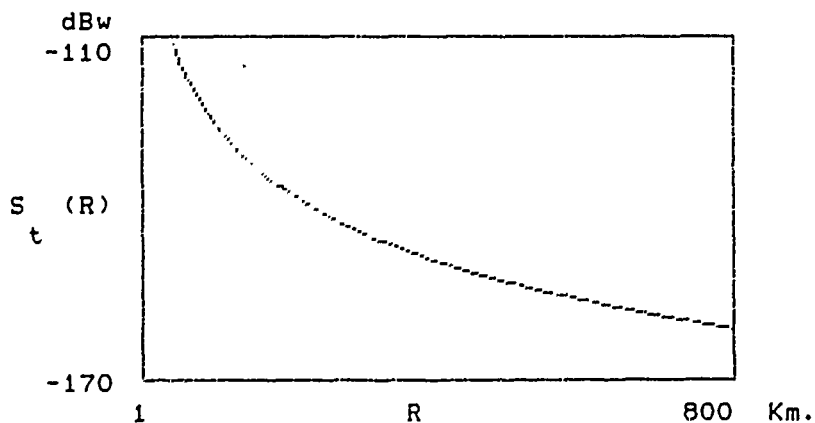
Signal power at Radar receiver :

$$S_t(R) := 10 \cdot \log \left[\frac{P_t^2 \cdot G_t^2 \cdot \sigma \cdot \lambda^4 \cdot g^4}{(4 \cdot \pi)^3 \cdot (1000 \cdot R)^4 \cdot L_t^4} \right] \quad (\text{in dBw})$$

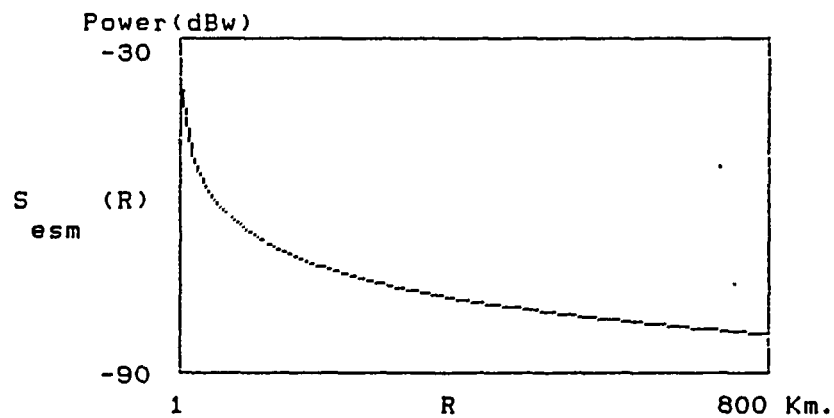
$$S_{t1}(R) := \frac{P_t^2 \cdot G_t^2 \cdot \sigma \cdot \lambda^4 \cdot g^4}{(4 \cdot \pi)^3 \cdot (1000 \cdot R)^4 \cdot L_t^4} \quad (\text{in Watts})$$

Signal power at ESM receiver (in dBw):

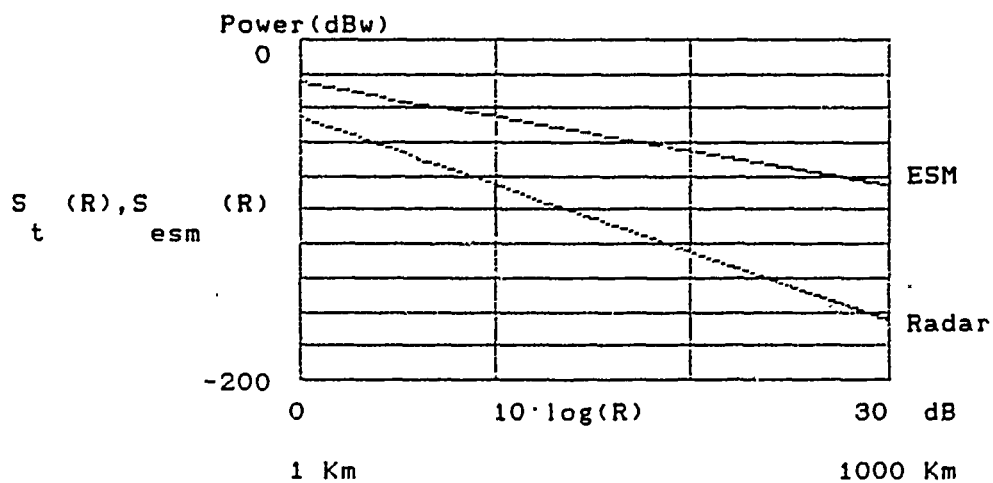
$$S_{esm}(R) := 10 \cdot \log \left[\frac{4 \cdot \pi \cdot G_{esm} \cdot (1000 \cdot R)^2}{\sigma \cdot G_t^2 \cdot g^2 \cdot L_t^2 \cdot L_{esm}} \right] \cdot S_{t1}(R)$$



Power at Radar receiver vs. Range



Power at ESM receiver vs. Range



Radar and ESM Power at reception comparison vs. Range (log scale) for the prescribed conditions ($\sigma = 20 \text{ m}^2$).

$$\text{Noise floor} = k T B_n F_n$$

ESM noise floor app. -98 dBw for an IFM

Radar noise floor app. -125 dBw (typical)

RADAR AND ESM MAXIMUM DET. RANGES AS FUNCTION OF SENSITIVITY

a.- Radar maximum detection range

$k := 1.38 \cdot 10^{-23}$ J/deg Boltzman's constant

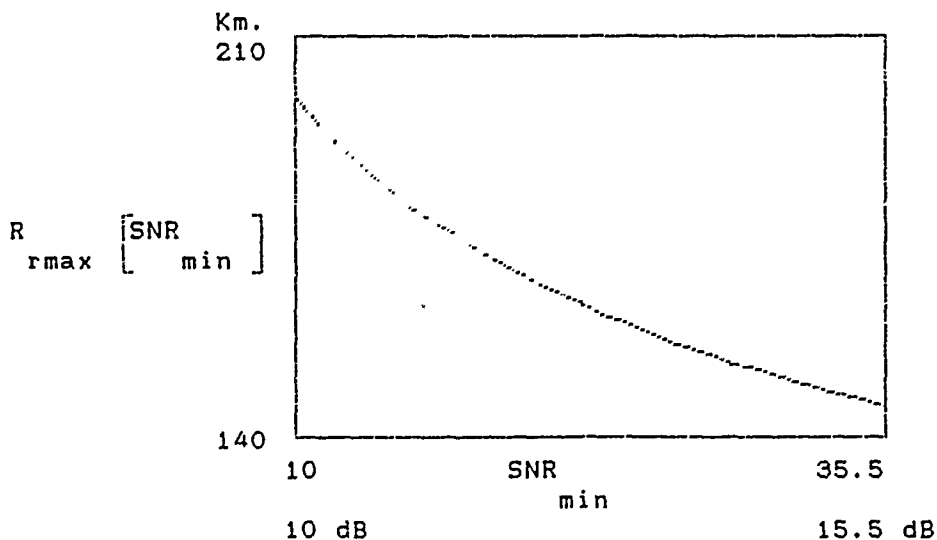
$T_o := 290$ Kelvin

$B_r := \frac{1}{r}$ Receiver Bandwidth

$SNR_{min} := 10, 10.5 \dots 35.5$ Minimum SNR reqd. for detection (10 to 15 dB)

$F := 4$ Noise Figure (6 dB)

$$R_{rmax} [SNR_{min}] := \left[\frac{P_t \cdot G_t^2 \cdot \lambda^2 \cdot \sigma_g^4}{(4 \cdot \pi)^3 \cdot k \cdot T_o \cdot B_r \cdot F \cdot SNR_{min}} \right]^{.25} \cdot 10^{-3}$$



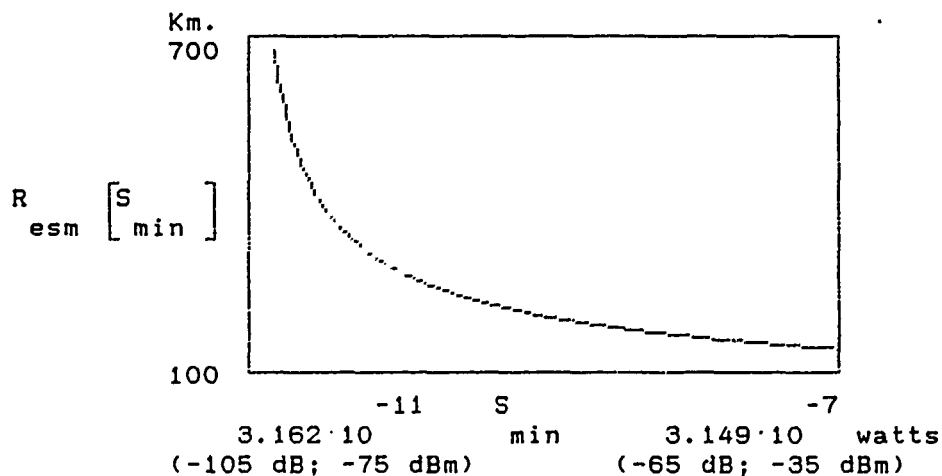
Radar maximum detection range as function of SNR

b.- ESM receiver maximum detection range (this is minimum signal required above the noise floor to in order to generate a detection.

Sensitivity range -105 to -65 dBw (-75 to -35 dBm):

$$S_{\min} := 3.162 \cdot 10^{-11}, 20 \cdot 10^{-10} \dots 3.162 \cdot 10^{-7}$$

$$R_{\text{esm}} [S_{\min}] := \left[\frac{P_t \cdot G_t \cdot G_{\text{esm}} \cdot \lambda^2}{(4 \cdot \pi)^2 \cdot S_{\min} \cdot L_t \cdot L_{\text{esm}}} \right]^{.5} \cdot 10^{-3}$$



ESM performance in range for detection of a radar main lobe as a function of various sensitivity levels.

2.- FLIGHT HEIGHT (ESM Rmax = Radar Horizon)

$$h_{\text{tKm}} := \frac{h_t}{1000} \quad \text{Radar height (Km)}$$

$$h_{\text{esmKm}} := \frac{h_{\text{esm}}}{1000} \quad \text{ESM aircraft height (Km)}$$

Sensitivity range, -105 dBw (-75 dBm) to -75 dBw (-45 dBm):

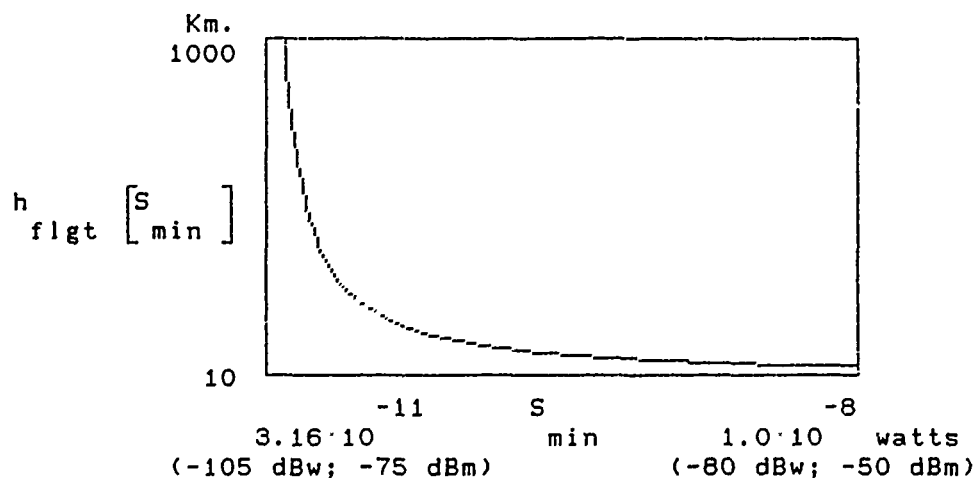
$$S_{\text{min}} := 3.16 \cdot 10^{-11}, 9.9 \cdot 10^{-11} \dots 3.16 \cdot 10^{-8}$$

Radar Horizon (Km) equation:

$$R_{\text{Hz}} := 130.34 \cdot \left[\left[h_{\text{esmKm}} \right]^{.5} + \left[h_{\text{tKm}} \right]^{.5} \right]$$

Then the height in Kilometers will be found from:

$$h_{\text{flgt}} \left[\begin{matrix} S \\ \text{min} \end{matrix} \right] := \left[7.672 \cdot 10^{-6} \cdot \frac{P_t \cdot G_t \cdot G_{\text{esm}} \cdot \lambda^2}{(4 \cdot \pi)^2 \cdot S_{\text{min}} \cdot L_t \cdot L_{\text{esm}}} - \left[h_{\text{tKm}} \right]^2 \right]^2$$

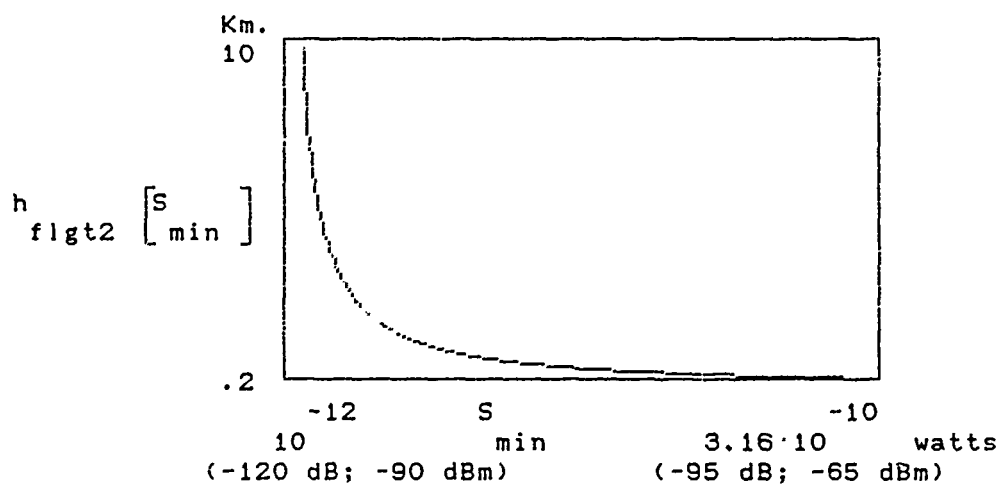


Flight height (in Km) for detecting the Radar's main lobe (Gt = 1585) vs. various Sensitivity levels.

For side lobes detection, ($G_t = 0.5$) :

$$S_{\min} := 1 \cdot 10^{-12}, 2 \cdot 10^{-12} \dots 3.16227 \cdot 10^{-10}$$

$$h_{\text{flgt2}} [S_{\min}] := \left[7.672 \cdot 10^{-6} \cdot \left(\frac{P_t \cdot 0.5 \cdot G_{\text{esm}} \cdot \lambda^2}{(4 \cdot \pi)^2 \cdot S_{\min} \cdot L_t \cdot L_{\text{esm}}} \right) - \sqrt{\frac{h}{t \text{ Km}}} \right]^2$$



Flight height (in Km.) for detecting the Radar's sidelobes ($G_t = 0.5$) vs. various sensitivity levels

APPENDIX B: SETUP (SUPERHET)

Superhet Receiver case

In this file the user must state the required parameters for both the ESM receiver and the enemy Radar to be encountered.

The follow on calculations will automatically update their output every time a change is made.

SHIPBORNE ENEMY RADAR (AIR SURVEILLANCE)

hr := 20	Enemy radar height (m)
Pt := 250000	Peak power (watts)
$ft := 3 \cdot 10^9$	Center frequency (Hz)
$\lambda_t := \frac{3 \cdot 10^8}{ft}$	Transmitter wavelength
Gtml := 1585	Gain Radar Main Lobe (32 dB)
Gtsl := .5	Gain Radar Side lobe (-3 dB)
PRF := 300	Pulse Repetition Frequency (Hz)
$PRI := \frac{1}{PRF}$	Pulse Repetition Interval
$PW := 4 \cdot 10^{-6}$	Pulse width (sec)
Lt := 3	Radar transmission losses
g := 1	Multipath factor $0 < g^2 < 4$
RPM := 6	Antenna Scan Rate
B3dB := 2.5	Antenna 3dB Beamwidth
$Ta := \frac{60}{RPM}$	Period of Antenna Scan

$$r_a := \frac{83\text{dB}}{360} \cdot T_a$$

Time Antenna's Main Lobe Points
in a particular direction

ESM RECEIVER PARAMETERS

$$V_{mph} := 220$$

ESM platform speed (knots)

$$V_m := V_{mph} \cdot .447$$

ESM platform speed (m/sec)

$$h_{esm} := 4000$$

Height of ESM platform (m)

$$F_L := 2.0 \cdot 10^9$$

Minimum Frequency (Hz)

$$F_U := 4.0 \cdot 10^9$$

Upper Frequency (Hz)

$$D := F_U - F_L$$

Frequency Band of Coverage

$$B_r := 50 \cdot 10^6$$

RF Bandwidth (Hz)

$$B_v := 10 \cdot 10^6$$

Video Bandwidth (Hz)

$$B_a := 50 \cdot 10^6$$

Acceptance Bandwidth (Hz)

$$\Gamma := \frac{B_r}{B_v}$$

Ratio of B_r to B_v

$$\text{gamma} := .8$$

Integration efficiency coeff.

$$PG := \left[\frac{B_r}{2 \cdot B_v} \right]^{\text{gamma}}$$

Processing Gain

$$F_n := 10$$

Receiver Noise Figure (in dB)

$$FN := \frac{F_n}{10}$$

Receiver Noise Figure

$$G_{esm} := 1$$

ESM Antenna Gain

$$P_{fa} := 1 \cdot 10^{-11}$$

Probability of False Alarm

Lesm := 3

Receiver internal losses

$$Ts := \frac{5 \cdot D}{\left[Ba + \frac{1}{PW} \right] \cdot PRF}$$

Time to scan Frequency band
(sec.)

$$rf := \frac{\left[Ba + \frac{1}{PW} \right]}{D} \cdot Ts$$

Time a particular frequency
remains in the Receiver Passband

$$d := \frac{PW}{2}$$

Minimum coincidence duration

T := 10

Time increment (sec)

tf := 220

Increment limit

Esm and Radar input parameters are written into output files
called ESM and RADAR respectively.

i := 1 ..14

j := 1 ..22

Radar :=
i

hr
Pt
ft
ht
Gtmi
Gtsi
PRF
PRI
PW
g
ESdB
Ta
ra
Lt

ESM :=
j

Vmph
Vm
hesm
FL
FU
D
Br
Bv
Ba
r
gamma
PG
Fn
FN
Gesm
Pfa
Lesm
Ts
rf
d
T
tf

WRITEPRN [Radar
prn] := Radar
i

WRITEPRN [ESM
prn] := ESM
j

APPENDIX C: SETUP (IFM)

IFM based ESM Receiver case

In this file the user must state the required parameters for both the IFM based ESM receiver and the enemy Radar to be encountered. The follow on calculations will automatically update their output every time a change is made.

SHIPBORNE ENEMY RADAR (AIR SURVEILLANCE)

hr := 20	Enemy radar height (m)
Pt := 250000	Peak power (watts)
ft := $3 \cdot 10^9$	Center frequency (Hz)
$\lambda_t := \frac{3 \cdot 10^8}{ft}$	Transmitter wavelength
Gtml := 1585	Gain Radar Main Lobe (app 32 dB)
Gtsl := .5	Gain Radar Side lobe (app -3 dB)
PRF := 300	Pulse Repetition Frequency (Hz)
$PRI := \frac{1}{PRF}$	Pulse Repetition Interval
PW := $4 \cdot 10^{-6}$	Pulse width (sec)
Lt := 3	Radar transmission losses
g := 1	Multipath factor $0 < g^2 < 4$
RPM := 6	Antenna Scan Rate
$\theta_{3dB} := 2.5$	Antenna 3dB Beamwidth

$$T_a := \frac{60}{\text{RPM}}$$

Period of Antenna Scan

$$\tau_a := \frac{93\text{dB}}{360} T_a$$

Time Antenna's Main Lobe Points
in a particular direction

ESM RECEIVER PARAMETERS

$$V_{\text{mph}} := 220$$

ESM platform speed (knots)

$$V_m := V_{\text{mph}} : 447$$

ESM platform speed (m/sec)

$$h_{\text{esm}} := 4000$$

Height of ESM platform (m)

$$F_L := 2.0 \cdot 10^9$$

Minimum Frequency (Hz)

$$F_U := 4.0 \cdot 10^9$$

Upper Frequency (Hz)

$$D := F_U - F_L$$

Frequency Band of Coverage

$$B_r := 2000 \cdot 10^6$$

RF Bandwidth (Hz)

$$B_v := 10 \cdot 10^6$$

Video Bandwidth (Hz)

$$B_a := 2000 \cdot 10^6$$

Acceptance Bandwidth (Hz)

$$\Gamma := \frac{B_r}{B_v}$$

Ratio of B_r to B_v

$$\text{gamma} := .5$$

Integration efficiency coefficient

$$P_G := \left[\frac{B_r}{2 \cdot B_v} \right]^{\text{gamma}}$$

Processing Gain

$$F_n := 15$$

Receiver Noise Figure (in dB)

$$F_N := 10^{\frac{F_n}{10}}$$

Receiver Noise Figure

Gesm := 1
 -11
Pfa := 1·10

Lesm := 3

PW
d := $\frac{\text{PW}}{2}$

T := 10

tf := 220

ESM Antenna Gain (Omni)

Probability of False Alarm

Receiver internal losses

Minimum coincidence duration

Time increment (sec)

Increment limit

Esm and Radar input parameters are written into output files called ESM and RADAR respectively.

i := 1 ..14

Radar :=
i

hr
Pt
ft
λ t
Gtml
Gtsl
PRF
PRI
PW
g
@3dB
Ta
ra
Lt

j := 1 ..20

ESMifm :=
j

Vmph
Vm
hesm
FL
FU
D
Br
Bv
Ba
Γ
gamma
PG
Fn
FN
Gesm
Pfa
Lesm
d
T
tf

WRITEPRN [Radar
prn] := Radar
i

WRITEPRN [ESMifm
prn] := ESMifm
j

APPENDIX D: PROBABILITY OF DETECTION (SUPERHET)

Superhet Receiver case

This file calculates the probability of detection for a general ESM System based on the theory explained in Tsui's book [Ref. 3], that is, considering the effects of the ratio B_r to B_v .

```
Radar := READPRN [ Radar  
                  prn ]
```

```
ESM := READPRN [ ESM  
                 prn ]
```

RADAR PARAMETERS

```
hr := Radar  
    0  
Pt := Radar  
    1  
ft := Radar  
    2  
 $\lambda$  := Radar  
    3  
Gtml := Radar  
    4  
Gtsl := Radar  
    5  
PRF := Radar  
    6  
PRI := Radar  
    7  
PW := Radar  
    8  
g := Radar  
    9  
B3dB := Radar  
    10  
Ta := Radar  
    11  
ra := Radar  
    12  
Lt := Radar  
    13
```

ESM RECEIVER PARAMETERS

```

Vmph := ESM
0
Vm := ESM
1
hesm := ESM
2
FL := ESM
3
FU := ESM
4
D := ESM
5
Br := ESM
6
Bv := ESM
7
Ba := ESM
8
Γ := ESM
9
gamma := ESM
10
PG := ESM
11
Fn := ESM
12
FN := ESM
13
Gesm := ESM
14
Pfa := ESM
15
Lesm := ESM
16
Ts := ESM
17
rF := ESM
18
d := ESM
19
T := ESM
20
tf := ESM
21

```

Range Calculations

$$ae := 8493.3 \cdot 10^3 \quad \text{Earth Radius (m)}$$

$$t := 0,1 \dots tf$$

$$t1_t := T \cdot t \quad hr_{Km} := \frac{hr}{1000} \quad hesm_{Km} := \frac{hesm}{1000}$$

$$R1 := ae + hr$$

$$R2 := ae + hesm$$

Maximum Range (Radar Horizon):

$$Rmax := 130.34 \cdot 10^3 \cdot \left[\sqrt{\frac{hesm}{Km}} + \sqrt{\frac{hr}{Km}} \right] \quad (d-1)$$

Maximum Range Angle:

$$\theta_{rad} := \arccos \left[\frac{Rmax^2 - R1^2 - R2^2}{-2 \cdot R1 \cdot R2} \right] \quad (d-2)$$

$$\theta_t := \left[\frac{t1}{Vm \cdot R1} \right] \quad \text{Range Angle Increment} \quad (d-3)$$

LOS Range Increment:

$$R_t := \sqrt{R1^2 + R2^2 - [2 \cdot R1 \cdot R2 \cdot \cos[\theta_{rad} - \theta_t]]} \quad (d-4)$$

$$G_t := \sqrt{R_t^2 - hesm} \quad \text{Ground Range increment} \quad (d-5)$$

SIGNAL TO NOISE RATIO CALCULATIONS

$$k := 1.38 \cdot 10^{-23}$$

Boltzman's constant

$$T_o := 290$$

Standard Temperature in Kelvin

$$B_{eff} := \frac{B_r}{\left[\frac{B_r}{2 \cdot B_v} \right]^{\gamma}}$$

Effective Bandwidth

(d-6)

$$N := k \cdot T_o \cdot B_r \cdot F_N$$

Receiver Noise Power

(d-7)

Main Lobe Signal to Noise Ratio:
(at output of detector)

Side Lobe Signal to Noise Ratio:
(at output of detector)

(d-8)

(d-9)

$$SNR_{ml_t} := \frac{G_{tml} \cdot P_t \cdot G_{esm} \cdot \lambda^2 \cdot g^2}{\left[4 \cdot \pi \cdot R_t \right]^2 \cdot N \cdot L_t \cdot L_{esm}}$$

$$SNR_{sl_t} := SNR_{ml_t} \cdot \left[\frac{G_{tsl}}{G_{tml}} \right]$$

PROBABILITY OF DETECTION CALCULATIONS

MAIN LOBE

SIDE LOBE

$$K_{im_t} := 1 + SNR_{ml_t} \quad (d-10)$$

$$K_{is_t} := 1 + SNR_{sl_t} \quad (d-11)$$

$$K2m_t := \frac{1}{\sqrt{1 + \frac{\Gamma^2}{2}}} \cdot \left[1 + \left[\text{SNRml}_t \cdot \frac{1 + \frac{\Gamma^2}{2}}{1 + \frac{\Gamma^2}{4}} \right] \right] \quad \text{Main lobe} \quad (d-12)$$

$$K2s_t := \frac{1}{\sqrt{1 + \frac{\Gamma^2}{2}}} \cdot \left[1 + \left[\text{SNRsl}_t \cdot \frac{1 + \frac{\Gamma^2}{2}}{1 + \frac{\Gamma^2}{4}} \right] \right] \quad \text{Side lobes} \quad (d-13)$$

$$K3m_t := \frac{4}{2 + 3 \cdot \frac{\Gamma^2}{4}} \cdot \left[1 + \left[3 \cdot \text{SNRml}_t \cdot \frac{2 + 3 \cdot \frac{\Gamma^2}{4}}{2 + \frac{\Gamma^2}{4}} \right] \right] \quad \text{Main lobe} \quad (d-14)$$

$$K3s_t := \frac{4}{2 + 3 \cdot \frac{\Gamma^2}{4}} \cdot \left[1 + \left[3 \cdot \text{SNRsl}_t \cdot \frac{2 + 3 \cdot \frac{\Gamma^2}{4}}{2 + \frac{\Gamma^2}{4}} \right] \right] \quad \text{Side lobes} \quad (d-15)$$

MAIN LOBE

$$K4m_t := \frac{K1m_t^2}{K2m_t} \quad (d-16)$$

(d-18)

$$K5m_t := \frac{\sqrt{-2 \cdot \ln(Pfa) - K1m_t}}{\sqrt{K2m_t}}$$

SIDE LOBES

$$K4s_t := \frac{K1s_t^2}{K2s_t} \quad (d-17)$$

(d-19)

$$K5s_t := \frac{\sqrt{-2 \cdot \ln(Pfa) - K1s_t}}{\sqrt{K2s_t}}$$

$$Xm_t := \frac{1}{\sqrt{2 \cdot \pi}} \cdot \frac{K3m_t}{6 \cdot \sqrt{K2m_t^3}} \cdot [K4m_t - 1] \cdot \exp \left[\max \left[\left[\frac{-K4m_t}{2} \right], \left[\frac{-500}{-500} \right] \right] \right] \quad (d-20)$$

$$Xs_t := \frac{1}{\sqrt{2 \cdot \pi}} \cdot \frac{K3s_t}{6 \cdot \sqrt{K2s_t^3}} \cdot [K4s_t - 1] \cdot \exp \left[\max \left[\left[\frac{-K4s_t}{2} \right], \left[\frac{-500}{-500} \right] \right] \right] \quad (d-21)$$

$$Ym_t := \frac{1}{\sqrt{2 \cdot \pi}} \cdot \frac{K3m_t}{6 \cdot \sqrt{K2m_t^3}} \cdot [K5m_t^2 - 1] \cdot \exp \left[\max \left[\left[\frac{-K5m_t^2}{2} \right], \left[\frac{-500}{-500} \right] \right] \right] \quad (d-22)$$

$$Y_{s_t} := \frac{1}{\sqrt{2 \cdot \pi}} \cdot \frac{K3s_t}{6 \cdot \sqrt[3]{K2s_t}} \cdot \left[K5s_t^2 - 1 \right] \cdot \exp \left[\max \left[\begin{array}{c} \frac{-K5s_t^2}{2} \\ -500 \end{array} \right] \right] \quad (d-23)$$

$$A_{m_t} := X_{m_t} + \left[\frac{1}{2} - \frac{1}{2} \cdot \operatorname{erf} \left[-\frac{\sqrt{K4m_t}}{\sqrt{2}} \right] \right] \quad (d-24)$$

$$A_{s_t} := X_{s_t} + \left[\frac{1}{2} - \frac{1}{2} \cdot \operatorname{erf} \left[-\frac{\sqrt{K4s_t}}{\sqrt{2}} \right] \right] \quad (d-25)$$

$$B_{m_t} := Y_{m_t} + \left[\frac{1}{2} - \frac{1}{2} \cdot \operatorname{erf} \left[\frac{\sqrt{K5m_t}}{\sqrt{2}} \right] \right] \quad (d-26)$$

$$B_{s_t} := Y_{s_t} + \left[\frac{1}{2} - \frac{1}{2} \cdot \operatorname{erf} \left[\frac{\sqrt{K5s_t}}{\sqrt{2}} \right] \right] \quad (d-27)$$

$$C_{m_t} := -Y_{m_t} + X_{m_t} + \frac{1}{2} \cdot \operatorname{erf} \left[\frac{\sqrt{K5m_t}}{\sqrt{2}} \right] - \frac{1}{2} \cdot \operatorname{erf} \left[-\frac{\sqrt{K4m_t}}{\sqrt{2}} \right] \quad (d-28)$$

$$Cs_t := -Ys_t + Xs_t + \frac{1}{2} \cdot \text{erf} \left[\frac{K5s_t}{\sqrt{2}} \right] - \frac{1}{2} \cdot \text{erf} \left[-\frac{K4s_t}{\sqrt{2}} \right] \quad (d-29)$$

$$Pd1m_t := \frac{Bm_t}{Am_t} \quad (d-30)$$

$$Pd1s_t := \frac{Bs_t}{As_t} \quad (d-31)$$

$$Pd2m_t := \frac{Am_t - Cm_t}{Am_t} \quad (d-32)$$

$$Pd2s_t := \frac{As_t - Cs_t}{As_t} \quad (d-33)$$

$$Pdm_t := Pd1m_t \cdot \mathbb{I} \left[.5 - Pd1m_t \right] + Pd2m_t \cdot \mathbb{I} \left[Pd2m_t - .5 \right] \quad (d-34)$$

$$Pds_t := Pd1s_t \cdot \mathbb{I} \left[.5 - Pd1s_t \right] + Pd2s_t \cdot \mathbb{I} \left[Pd2s_t - .5 \right] \quad (d-35)$$

The values for the Probability of Detection vs. time are written into output files.

$$\text{WRITEPRN} \left[Pdgm_{prn} \right] := Pdm_t$$

$$\text{WRITEPRN} \left[Pdgs_{prn} \right] := Pds_t$$

APPENDIX E: PROBABILITY OF DETECTION (IFM)

IFM based Receiver case

This file calculates the probability of detection for a general ESM System based on the theory explained in Tsui's book, that is, considering the effects of the ratio B_r to B_v .

```
Radar := READPRN [ Radar  
                  prn ]
```

```
ESMifm := READPRN [ ESMifm  
                   prn ]
```

RADAR PARAMETERS

```
hr := Radar  
    0  
Pt := Radar  
    1  
ft := Radar  
    2  
 $\lambda$  := Radar  
    3  
Gtml := Radar  
    4  
Gtsl := Radar  
    5  
PRF := Radar  
    6  
PRI := Radar  
    7  
PW := Radar  
    8  
g := Radar  
    9  
B3dB := Radar  
    10  
Ta := Radar  
    11  
ra := Radar  
    12  
Lt := Radar  
    13
```

ESM RECEIVER PARAMETERS

```

Vmph := ESMifm
      0
Vm := ESMifm
    1
hesm := ESMifm
      2
FL := ESMifm
    3
FU := ESMifm
    4
D := ESMifm
    5
Br := ESMifm
    6
Bv := ESMifm
    7
Ba := ESMifm
    8
Γ := ESMifm
    9
gamma := ESMifm
      10
PG := ESMifm
    11
Fn := ESMifm
    12
FN := ESMifm
    13
Gesm := ESMifm
      14
Pfa := ESMifm
    15
Lesm := ESMifm
    16
d := ESMifm
    17
T := ESMifm
    18
tf := ESMifm
    19

```

```

ae := 8493.3*103                                Earth Radius (m)
t := 0,1 ..tf
t1 := T*t
t      hr      hr      hesm      hesm
      Km      := 1000      Km      1000
R1 := ae + hr
R2 := ae + hesm

```

$$R_{\max} := 130.34 \cdot 10^3 \cdot \left[\sqrt{\frac{\text{hesm}}{\text{Km}}} + \sqrt{\frac{\text{hr}}{\text{Km}}} \right] \quad (e-1)$$
$$\text{Erad} := \text{acos} \left[\frac{R_{\text{max}}^2 - R_1^2 - R_2^2}{-2 \cdot R_1 \cdot R_2} \right] \quad (\text{e-2})$$
$$\Theta_t := \left[V_m \frac{t_1}{R_1} \right] \quad (e-3)$$
$$R_t := \sqrt{R_1^2 + R_2^2 - 2 \cdot R_1 \cdot R_2 \cdot \cos[\theta_{rad} - \theta_t]} \quad (e-4)$$

SIGNAL TO NOISE RATIO CALCULATIONS

$$k := 1.38 \cdot 10^{-23}$$

Boltzman's constant

$$T_o := 290$$

Standard Temperature in Kelvin

Receiver effective Bandwidth:

$$B_{eff} := \frac{B_r}{\left[\frac{B_r}{2 \cdot B_v} \right]^{\gamma}} \quad (e-5)$$

Receiver Noise Power:

$$N := k \cdot T_o \cdot B_r \cdot F_N \quad (e-6)$$

Main Lobe Signal to Noise Ratio
(at output of detector):

(e-7)

Side Lobe Signal to Noise Ratio
(at output of detector):

(e-8)

$$SNR_{ml_t} := \frac{G_{tml} \cdot P_t \cdot G_{esm} \cdot \lambda^2 \cdot g^2}{\left[4 \cdot \pi \cdot R_t \right]^2 \cdot N \cdot L_t \cdot L_{esm}}$$

$$SNR_{sl_t} := SNR_{ml_t} \cdot \left[\frac{G_{tsl}}{G_{tml}} \right]$$

PROBABILITY OF DETECTION CALCULATIONS

MAIN LOBE

SIDE LOBE

$$K1m_t := 1 + SNRm1_t \quad (e-9)$$

$$K1s_t := 1 + SNRs1_t \quad (e-10)$$

$$K2m_t := \frac{1}{\sqrt{1 + \frac{\Gamma^2}{2}}} \left[1 + SNRm1_t \cdot \frac{1 + \frac{\Gamma^2}{2}}{1 + \frac{\Gamma^2}{4}} \right] \quad \text{Main lobe} \quad (e-11)$$

$$K2s_t := \frac{1}{\sqrt{1 + \frac{\Gamma^2}{2}}} \left[1 + SNRs1_t \cdot \frac{1 + \frac{\Gamma^2}{2}}{1 + \frac{\Gamma^2}{4}} \right] \quad \text{Side lobes} \quad (e-12)$$

$$K3m_t := \frac{4}{2 + 3 \cdot \frac{\Gamma^2}{4}} \left[1 + 3 \cdot SNRm1_t \cdot \frac{2 + 3 \cdot \frac{\Gamma^2}{4}}{2 + \frac{\Gamma^2}{4}} \right] \quad \text{Main lobe} \quad (e-13)$$

$$K3s_t := \frac{4}{2 + 3 \cdot \frac{\Gamma^2}{4}} \cdot \left[1 + \left[3 \cdot SNRs_t \cdot \frac{2 + 3 \cdot \frac{\Gamma^2}{4}}{2 + \frac{\Gamma^2}{4}} \right] \right] \quad \text{Side lobes (e-14)}$$

MAIN LOBE

SIDE LOBES

$$K4m_t := \frac{K1m_t^2}{K2m_t} \quad (e-15)$$

$$K4s_t := \frac{K1s_t^2}{K2s_t} \quad (e-16)$$

(e-17)

(e-18)

$$K5m_t := \frac{\sqrt{-2 \cdot \ln(Pfa) - K1m_t}}{\sqrt{K2m_t}}$$

$$K5s_t := \frac{\sqrt{-2 \cdot \ln(Pfa) - K1s_t}}{\sqrt{K2s_t}}$$

$$Xm_t := \frac{1}{\sqrt{2 \cdot \pi}} \cdot \frac{K3m_t}{6 \cdot \sqrt[3]{K2m_t}} \cdot [K4m_t - 1] \cdot \exp \left[\max \left[\frac{-K4m_t}{2}, -500 \right] \right] \quad (e-19)$$

$$Xs_t := \frac{1}{\sqrt{2 \cdot \pi}} \cdot \frac{K3s_t}{6 \cdot \sqrt[3]{K2s_t}} \cdot [K4s_t - 1] \cdot \exp \left[\max \left[\frac{-K4s_t}{2}, -250 \right] \right] \quad (e-20)$$

Main lobe:

$$Y_{m_t} := \frac{1}{\sqrt{2 \cdot \pi}} \cdot \frac{K3_m t}{6 \cdot \sqrt[3]{K2_m t}} \cdot \left[K5_m^2 t - 1 \right] \cdot \exp \left[\max \left[\frac{-K5_m^2 t}{2}, -500 \right] \right] \quad (e-21)$$

Side lobes:

$$Y_{s_t} := \frac{1}{\sqrt{2 \cdot \pi}} \cdot \frac{K3_s t}{6 \cdot \sqrt[3]{K2_s t}} \cdot \left[K5_s^2 t - 1 \right] \cdot \exp \left[\max \left[\frac{-K5_s^2 t}{2}, -500 \right] \right] \quad (e-22)$$

$$A_{m_t} := X_{m_t} + \left[\frac{1}{2} - \frac{1}{2} \cdot \operatorname{erf} \left[\frac{\sqrt{K4_m t}}{\sqrt{2}} \right] \right] \quad \text{Main lobe} \quad (e-23)$$

$$A_{s_t} := X_{s_t} + \left[\frac{1}{2} - \frac{1}{2} \cdot \operatorname{erf} \left[\frac{\sqrt{K4_s t}}{\sqrt{2}} \right] \right] \quad \text{Side lobes} \quad (e-24)$$

$$B_{m_t} := Y_{m_t} + \left[\frac{1}{2} - \frac{1}{2} \cdot \operatorname{erf} \left[\frac{\sqrt{K5_m t}}{\sqrt{2}} \right] \right] \quad \text{Main lobe} \quad (e-25)$$

$$B_{s_t} := Y_{s_t} + \left[\frac{1}{2} - \frac{1}{2} \cdot \operatorname{erf} \left[\frac{\sqrt{K5_s t}}{\sqrt{2}} \right] \right] \quad \text{Side lobes} \quad (e-26)$$

Main lobe:

$$Cm_t := -Ym_t + Xm_t - \frac{1}{2} \cdot \text{erf} \left[-\frac{\sqrt{K4m}}{\sqrt{2}} \frac{t}{t} \right] + \frac{1}{2} \cdot \text{erf} \left[\frac{\sqrt{K5m}}{\sqrt{2}} \frac{t}{t} \right] \quad (e-27)$$

Side lobes:

$$Cs_t := -Ys_t + Xs_t - \frac{1}{2} \cdot \text{erf} \left[-\frac{\sqrt{K4s}}{\sqrt{2}} \frac{t}{t} \right] + \frac{1}{2} \cdot \text{erf} \left[\frac{\sqrt{K5s}}{\sqrt{2}} \frac{t}{t} \right] \quad (e-28)$$

$$Pd1m_t := \frac{Bm_t}{Am_t} \quad (e-29)$$

$$Pd1s_t := \frac{Bs_t}{As_t} \quad (e-30)$$

$$Pd2m_t := \frac{Am_t - Cm_t}{Am_t} \quad (e-31)$$

$$Pd2s_t := \frac{As_t - Cs_t}{As_t} \quad (e-32)$$

Main lobe probability of detection (IFM System):

$$PdmIFM_t := Pd1m_t \cdot \bar{x} \left[.5 - Pd1m_t \right] + Pd2m_t \cdot \bar{x} \left[Pd2m_t - .5 \right] \quad (e-33)$$

Side lobes probability of detection (IFM System):

$$PdsIFM_t := Pd1s_t \cdot \bar{x} \left[.5 - Pd1s_t \right] + Pd2s_t \cdot \bar{x} \left[Pd2s_t - .5 \right] \quad (e-34)$$

The probability of detection vs. time is written into an output file:

WRITEPRN $\begin{bmatrix} \text{PdgmIFM} \\ \text{prn} \end{bmatrix} := \text{PdmIFM}_t$ Main lobe

WRITEPRN $\begin{bmatrix} \text{PdgsIFM} \\ \text{prn} \end{bmatrix} := \text{PdsIFM}_t$ Side lobes

APPENDIX F: PROBABILITY OF IDENTIFICATION (SUPERHET)

Superhet Receiver case

This file calculates the probability of identification as a function of time $P_i(t)$ for a Superhet ESM System based on the percent error deviations of the input signal in angle of arrival, frequency, pulse repetition interval, and pulse width.

It reads the Radar and ESM parameters from the Radar/ESM parameter file and creates plots of $P_i(t)$ of both the emitter side lobes and main lobe. The file writes $P_i(t)$ data into an output file for the final $POI(t)$ calculations.

```
Radar := READPRN [ Radar  
                  prn ]
```

```
ESM := READPRN [ ESM  
                 prn ]
```

RADAR PARAMETERS

```
hr := Radar  
    0  
Pt := Radar  
    1  
ft := Radar  
    2  
 $\lambda$  := Radar  
    3  
Gtml := Radar  
    4  
Gtsl := Radar  
    5  
PRF := Radar  
    6  
PRI := Radar  
    7  
PW := Radar  
    8  
g := Radar  
    9  
E3dB := Radar  
    10
```

Ta := Radar
 11
 ra := Radar
 12
 Lt := Radar
 13

ESM RECEIVER PARAMETERS

Vmph := ESM
 0
 Vm := ESM
 1
 hesm := ESM
 2
 FL := ESM
 3
 FU := ESM
 4
 D := ESM
 5
 Br := ESM
 6
 Bv := ESM
 7
 Ba := ESM
 8
 F := ESM
 9
 gamma := ESM
 10
 PG := ESM
 11
 Fn := ESM
 12
 FN := ESM
 13
 Gesm := ESM
 14
 Pfa := ESM
 15
 Lesm := ESM
 16
 Ts := ESM
 17
 rF := ESM
 18
 d := ESM
 19

```
T := ESM
20
tf := ESM
21
```

Range Calculations

```
ae := 8493.3*103      Earth Radius (m)
```

$$t := 0, 1 \dots tf$$
$$t1_t := T \cdot t \qquad hr_{Km} := \frac{hr}{1000} \qquad hesm_{Km} := \frac{hesm}{1000}$$
$$R1 := ae + hr$$
$$R2 := ae + herm$$

Maximum Range (Radar Horizon):

$$R_{\max} := 130.34 \cdot 10^3 \cdot \left[\frac{h_{\text{esm}}}{K_m} + \frac{h_r}{K_m} \right] \quad (f-1)$$

Maximum Range Angle:

$$\Theta_{rad} := \arccos \left[\frac{R_{max}^2 - R_1^2 - R_2^2}{-2 \cdot R_1 \cdot R_2} \right] \quad (f-2)$$

Range Angle Increment:

$$E_t := \begin{bmatrix} t1 \\ t \\ Vm \cdot \frac{t}{R1} \end{bmatrix} \quad (f-3)$$

LOS Range Increment:

$$R_t = \sqrt{R_1^2 + R_2^2 - [2 \cdot R_1 \cdot R_2 \cdot \cos [\theta_{rad} - \theta_t]]} \quad (f-4)$$

SIGNAL TO NOISE RATIO CALCULATIONS

$$k := 1.38 \cdot 10^{-23}$$

Boltzman's constant

$$T_o := 290$$

Std. Temperature in Kelvin

Effective Bandwidth:

$$B_{eff} := \frac{B_r}{\left[\frac{B_r}{2 \cdot B_v} \right]^{\gamma}} \quad (f-5)$$

Receiver Noise Power:

$$N := k \cdot T_o \cdot B_{eff} \cdot F_N \quad (f-6)$$

Main Lobe Signal to Noise Ratio
(at output of detector)

(f-7)

$$SNR_{ml_t} := \frac{G_{tml} \cdot P_t \cdot G_{esm} \cdot \lambda^2 \cdot g^2}{\left[4 \cdot \pi \cdot R_t \right]^2 \cdot N \cdot L_t \cdot L_{esm}}$$

Side Lobe Signal to Noise Ratio
(at output of detector)

(f-8)

$$SNR_{sl_t} := SNR_{ml_t} \cdot \left[\frac{G_{tsl}}{G_{tml}} \right]$$

Main Lobe Signal Power
at Rx.:

(f-9)

$$S_{ml_t} := \frac{G_{tml} \cdot P_t \cdot G_{esm} \cdot \lambda^2 \cdot g^2}{\left[4 \cdot \pi \cdot R_t \right]^2 \cdot L_t \cdot L_{esm}}$$

Side Lobes Signal Power
at Rx.

(f-10)

$$S_{sl_t} := S_{ml_t} \cdot \left[\frac{G_{tsl}}{G_{tml}} \right]$$

PROBABILITY OF IDENTIFICATION CALCULATIONS

Frequency error (Main lobe and Side lobes):

$$dFm_t := \bar{x} \left[.001 - \frac{\max \left[4 \cdot \frac{\sqrt{3}}{\left[\frac{SNRm_l}{t} \cdot \pi \cdot PW \cdot B_{eff} \right]^2} \right]}{ft} \right] \quad (f-11)$$

$$dFs_t := \bar{x} \left[.001 - \frac{\max \left[4 \cdot \frac{\sqrt{3}}{\left[\frac{SNRs_l}{t} \cdot \pi \cdot PW \cdot B_{eff} \right]^2} \right]}{ft} \right] \quad (f-12)$$

Pulse Repetition interval error (Main lobe and Side lobes):

$$dPRIm_t := \bar{x} \left[.01 - 4 \cdot \frac{0.62 \cdot PRF}{B_v \cdot \left[\frac{SNRm_l}{t} \right]} \right] \quad (f-13)$$

$$dPRIs_t := \sqrt[3]{.01 - 4 \cdot \frac{0.62 \cdot PRF}{Bv \cdot \sqrt{SNRs1_t}}} \quad (f-14)$$

Pulse Width error (Main lobe and Side lobes):

$$dPWm_t := \sqrt[3]{.01 - \frac{4 \cdot \frac{.7}{Bv \cdot \sqrt{SNRm1_t}}}{PW}} \quad (f-15)$$

$$dPWs_t := \sqrt[3]{.01 - \frac{4 \cdot \frac{.7}{Bv \cdot \sqrt{SNRs1_t}}}{PW}} \quad (f-16)$$

Angle Of Arrival error:

$\theta_{rms} := 5$	Actual rms angular accuracy (degrees)
$\theta_{ref} := 4$	Angular accuracy of reference (degrees)
$Smin_{AOA} := 1.0 \cdot 10^{-8}$	Minimum discernible signal for the AOA receiving system (-80 dBw/-50 dBm)

$$dAOA_m_t := \left[\frac{4.0}{E_{rms}} \right] \cdot \bar{x} \left[S_{m1}_t - S_{min_AOA} \right] \quad (f-17)$$

$$dAOA_s_t := \left[\frac{4.0}{E_{rms}} \right] \cdot \bar{x} \left[S_{s1}_t - S_{min_AOA} \right] \quad (f-18)$$

Identification Matrix:

Each combination is properly weighed according to the quality of its components. The first coefficient is justified since each parameter has a relative importance, and therefore it defines the overall weight for each combination:

dAOA = 0.3
dF = 0.28
dPRI = 0.23
dPW = 0.19

And the second coefficient of each element of the matrix comes from the need to measure relative to a maximum value of 1 each of the combinations. Then if we just have obtained measurements from two or three parameters, only one combination will be selected.

w1 := 0.3	Weight corresponding to AOA error
w2 := 0.28	Weight corresponding to freq. error
w3 := 0.23	Weight corresponding to PRI error
w4 := 0.19	Weight corresponding to PW error

Main lobe probability of identification matrix:

(f-19)

$P_{im} := \max_t$

$$\begin{aligned}
 & \left[\begin{aligned}
 & 1 \cdot \left[0.25 \cdot \left[dAOAm_t + dFm_t + dPRIm_t + dPWm_t \right] \right] \\
 & \sqrt{w1 + w2 + w3} \cdot \left[0.333 \cdot \left[dAOAm_t + dFm_t + dPRIm_t \right] \right] \\
 & \sqrt{w1 + w2 + w4} \cdot \left[0.333 \cdot \left[dAOAm_t + dFm_t + dPWm_t \right] \right] \\
 & \sqrt{w1 + w3 + w4} \cdot \left[0.333 \cdot \left[dAOAm_t + dPRIm_t + dPWm_t \right] \right] \\
 & \sqrt{w2 + w3 + w4} \cdot \left[0.333 \cdot \left[dFm_t + dPRIm_t + dPWm_t \right] \right] \\
 & \sqrt{w1 + w2} \cdot \left[0.5 \cdot \left[dAOAm_t + dFm_t \right] \right] \\
 & \sqrt{w1 + w3} \cdot \left[0.5 \cdot \left[dAOAm_t + dPRIm_t \right] \right] \\
 & \sqrt{w1 + w4} \cdot \left[0.5 \cdot \left[dAOAm_t + dPWm_t \right] \right] \\
 & \sqrt{w2 + w3} \cdot \left[0.5 \cdot \left[dFm_t + dPRIm_t \right] \right] \\
 & \sqrt{w2 + w4} \cdot \left[0.5 \cdot \left[dFm_t + dPWm_t \right] \right] \\
 & \sqrt{w3 + w4} \cdot \left[0.5 \cdot \left[dPRIm_t + dPWm_t \right] \right] \\
 & \sqrt{w2} \cdot dFm_t \\
 & \sqrt{w3} \cdot dPRIm_t \\
 & \sqrt{w4} \cdot dPWm_t
 \end{aligned} \right]
 \end{aligned}$$

Side lobes probability of identification matrix:

(f-20)

$P_{is} := \max_t$

$$\begin{aligned}
 & 1 \cdot \left[0.25 \cdot \left[dAOAs_t + dFs_t + dPRIs_t + dPWs_t \right] \right] \\
 & \sqrt{w_1 + w_2 + w_3} \cdot \left[0.333 \cdot \left[dAOAs_t + dFs_t + dPRIs_t \right] \right] \\
 & \sqrt{w_1 + w_2 + w_4} \cdot \left[0.333 \cdot \left[dAOAs_t + dFs_t + dPWs_t \right] \right] \\
 & \sqrt{w_1 + w_3 + w_4} \cdot \left[0.333 \cdot \left[dAOAs_t + dPRIs_t + dPWs_t \right] \right] \\
 & \sqrt{w_2 + w_3 + w_4} \cdot \left[0.333 \cdot \left[dFs_t + dPRIs_t + dPWs_t \right] \right] \\
 & \sqrt{w_1 + w_2} \cdot \left[0.5 \cdot \left[dAOAs_t + dFs_t \right] \right] \\
 & \sqrt{w_1 + w_3} \cdot \left[0.5 \cdot \left[dAOAs_t + dPRIs_t \right] \right] \\
 & \sqrt{w_1 + w_4} \cdot \left[0.5 \cdot \left[dAOAs_t + dPWs_t \right] \right] \\
 & \sqrt{w_2 + w_3} \cdot \left[0.5 \cdot \left[dFs_t + dPRIs_t \right] \right] \\
 & \sqrt{w_2 + w_4} \cdot \left[0.5 \cdot \left[dFs_t + dPWs_t \right] \right] \\
 & \sqrt{w_3 + w_4} \cdot \left[0.5 \cdot \left[dPRIs_t + dPWs_t \right] \right] \\
 & \sqrt{w_2} \cdot dFs_t \\
 & \sqrt{w_3} \cdot dPRIs_t \\
 & \sqrt{w_4} \cdot dPWs_t
 \end{aligned}$$

The Probability of identification vs. time is written into an output file:

WRITEPRN $\begin{bmatrix} P_{idm} \\ prn \end{bmatrix} := P_{im} \quad t$

WRITEPRN $\begin{bmatrix} P_{ids} \\ prn \end{bmatrix} := P_{is} \quad t$

APPENDIX G: PROBABILITY OF IDENTIFICATION (IFM)

IFM based Receiver case

This file calculates the probability of identification as a function of time $P_i(t)$ for an IFM - ESM System based on the percent error deviations of the input signal in angle of arrival, frequency, pulse repetition interval, and pulse width.

It reads the Radar and ESM parameters from the Radar/ESM parameter file and creates plots of $P_i(t)$ of both the emitter sidelobes and mainlobe. The file writes $P_i(t)$ data into an output file for $POI(t)$ calculations.

```
Radar := READPRN [Radar  
                  prn ]
```

```
ESMifm := READPRN [ESMifm  
                   prn ]
```

RADAR PARAMETERS

```
hr := Radar  
    0  
Pt := Radar  
    1  
ft := Radar  
    2  
 $\lambda$  := Radar  
    3  
Gtml := Radar  
    4  
Gtsl := Radar  
    5  
PRF := Radar  
    6  
PRI := Radar  
    7  
PW := Radar  
    8  
g := Radar  
    9  
R3dB := Radar  
    10
```


Ta := Radar
 11
 ra := Radar
 12
 Lt := Radar
 13

ESM RECEIVER PARAMETERS

Vmph := ESMifm
 0
 Vm := ESMifm
 1
 hesm := ESMifm
 2
 FL := ESMifm
 3
 FU := ESMifm
 4
 D := ESMifm
 5
 Br := ESMifm
 6
 Bv := ESMifm
 7
 Ba := ESMifm
 8
 Γ := ESMifm
 9
 gamma := ESMifm
 10
 PG := ESMifm
 11
 Fn := ESMifm
 12
 FN := ESMifm
 13
 Gesm := ESMifm
 14
 Pfa := ESMifm
 15
 Lesm := ESMifm
 16
 d := ESMifm
 17
 T := ESMifm
 18
 tf := ESMifm
 19

Range Calculations

$$ae := 8493.3 \cdot 10^3 \quad \text{Earth Radius (m)}$$

$$t := 0, 1 \dots tf$$

$$t1_t := T \cdot t \quad hr_{Km} := \frac{hr}{1000} \quad hesm_{Km} := \frac{hesm}{1000}$$

$$R1 := ae + hr$$

$$R2 := ae + hesm$$

Maximum Range (Radar Horizon):

$$Rmax := 130.34 \cdot 10^3 \cdot \left[\sqrt{\frac{hesm}{Km}} + \sqrt{\frac{hr}{Km}} \right] \quad (g-1)$$

Maximum Range Angle:

$$\theta_{rad} := \arccos \left[\frac{Rmax^2 - R1^2 - R2^2}{-2 \cdot R1 \cdot R2} \right] \quad (g-2)$$

Range Angle Increment:

$$\theta_t := \left[\frac{t1}{R1} \right] \quad (g-3)$$

LOS Range Increment:

$$R_t := \sqrt{R1^2 + R2^2 - [2 \cdot R1 \cdot R2 \cdot \cos[\theta_{rad} - \theta_t]]} \quad (g-4)$$

SIGNAL TO NOISE RATIO CALCULATIONS

$$k := 1.38 \cdot 10^{-23}$$

Boltzman's constant

$$T_o := 290$$

Std. Temperature in Kelvin

Effective Bandwidth:

$$B_{eff} := \frac{B_r}{\left[\frac{B_r}{2 \cdot B_v} \right]^{gamma}} \quad (g-5)$$

Receiver Noise Power:

$$N := k \cdot T_o \cdot B_{eff} \cdot F_N \quad (g-6)$$

Main Lobe Signal to Noise Ratio
(at output of detector)

(g-7)

Side Lobe Signal to Noise Ratio
(at output of detector)

(g-8)

$$SNR_{ml_t} := \frac{G_{tml} \cdot P_t \cdot G_{esm} \cdot \lambda^2 \cdot g^2}{\left[4 \cdot \pi \cdot R_t \right]^2 \cdot N \cdot L_t \cdot L_{esm}}$$

$$SNR_{sl_t} := SNR_{ml_t} \cdot \left[\frac{G_{tsl}}{G_{tml}} \right]$$

Signal Power at ESM from Radar mainlobe :

(g-9)

Signal Power at ESM from Radar Side lobes :

(g-10)

$$S_{ml_t} := \frac{G_{tml} \cdot P_t \cdot G_{esm} \cdot \lambda^2 \cdot g^2}{\left[4 \cdot \pi \cdot R_t \right]^2 \cdot L_t \cdot L_{esm}}$$

$$S_{sl_t} := S_{ml_t} \cdot \left[\frac{G_{tsl}}{G_{tml}} \right]$$

PROBABILITY OF IDENTIFICATION CALCULATIONS

Frequency Resolution = 2 MHz. ; (11 bit word length)

⁶
R := 2 · 10

Frequency error (Main lobe and Side lobes) :

$$dF_{m_t} := \bar{x} \left[.001 - \frac{\max \left[4 \cdot \frac{\sqrt{3}}{\left[\frac{SNR_{m_t} \cdot \pi \cdot PW \cdot B_{eff}}{R} \right]} \right]}{ft} \right] \quad (g-11)$$

$$dF_{s_t} := \bar{x} \left[.001 - \frac{\max \left[4 \cdot \frac{\sqrt{3}}{\left[\frac{SNR_{s_t} \cdot \pi \cdot PW \cdot B_{eff}}{R} \right]} \right]}{ft} \right] \quad (g-12)$$

Pulse Repetition interval error (Main lobe and Side lobes):

$$dPRIm_t := \bar{x} \left[.01 - 4 \cdot \frac{0.62 \cdot PRF}{B_v \cdot \left[\frac{SNR_{m_t}}{t} \right]} \right] \quad (g-13)$$

$$dPRIs_t := \Xi \left[.01 - 4 \cdot \frac{0.62 \cdot PRF}{Bv \cdot \sqrt{SNRs1_t}} \right] \quad (g-14)$$

Pulse Width error (Main lobe and Side lobes):

$$dPWm_t := \Xi \left[.001 - \frac{4 \cdot \left[\frac{.7}{Bv \cdot \sqrt{SNRm1_t}} \right]}{PW} \right] \quad (g-15)$$

$$dPWs_t := \Xi \left[.001 - \frac{4 \cdot \left[\frac{.7}{Bv \cdot \sqrt{SNRs1_t}} \right]}{PW} \right] \quad (g-16)$$

Angle Of Arrival error:

$\theta_{rms} := 5$

Actual rms angular accuracy
(degrees)

$\theta_{ref} := 4$

Angular reference accuracy
(degrees)

$S_{min}^{AOA} := 1.0 \cdot 10^{-8}$

Minimum discernible signal
for the AOA receiving system
(-80 dBw or -50 dBm)

$$dAOA_{mt} := \left[\frac{4.0}{\sigma_{rms}} \right] \cdot \bar{x} \left[S_{mt} - S_{min\ AOA} \right] \quad (g-17)$$

$$dAOAs_t := \left[\frac{4.0}{\sigma_{rms}} \right] \cdot \bar{x} \left[S_{st} - S_{min\ AOA} \right] \quad (g-18)$$

Identification Matrix:

Each combination is properly weighed according to the quality of its components. The first coefficient is justified since each parameter has a relative importance, and therefore it defines the overall weight for each combination:

dAOA = 0.3
dF = 0.28
dPRI = 0.23
dPW = 0.19

And the second coefficient of each element of the matrix comes from the need to measure relative to a maximum value of 1 each of the combinations. Then if we just have obtained measurements from two or three parameters, only one combination will be selected.

w1 := 0.3	Weight corresponding to AOA error
w2 := 0.28	Weight corresponding to Freq. error
w3 := 0.23	Weight corresponding to PRI error
w4 := 0.19	Weight corresponding to PW error

Main lobe Probability of identification matrix:

(g-19)

$P_{im} := \max_t$

$$\begin{aligned}
 & 1 \cdot \left[0.25 \cdot \left[\begin{matrix} dA0Am_t & dFm_t & dPRIm_t & dPWm_t \end{matrix} \right] \right] \\
 & \sqrt{w1 + w2 + w3} \cdot \left[0.333 \cdot \left[\begin{matrix} dA0Am_t & dFm_t & dPRIm_t \end{matrix} \right] \right] \\
 & \sqrt{w1 + w2 + w4} \cdot \left[0.333 \cdot \left[\begin{matrix} dA0Am_t & dFm_t & dPWm_t \end{matrix} \right] \right] \\
 & \sqrt{w1 + w3 + w4} \cdot \left[0.333 \cdot \left[\begin{matrix} dA0Am_t & dPRIm_t & dPWm_t \end{matrix} \right] \right] \\
 & \sqrt{w2 + w3 + w4} \cdot \left[0.333 \cdot \left[\begin{matrix} dFm_t & dPRIm_t & dPWm_t \end{matrix} \right] \right] \\
 & \sqrt{w1 + w2} \cdot \left[0.5 \cdot \left[\begin{matrix} dA0Am_t & dFm_t \end{matrix} \right] \right] \\
 & \sqrt{w1 + w3} \cdot \left[0.5 \cdot \left[\begin{matrix} dA0Am_t & dPRIm_t \end{matrix} \right] \right] \\
 & \sqrt{w1 + w4} \cdot \left[0.5 \cdot \left[\begin{matrix} dA0Am_t & dPWm_t \end{matrix} \right] \right] \\
 & \sqrt{w2 + w3} \cdot \left[0.5 \cdot \left[\begin{matrix} dFm_t & dPRIm_t \end{matrix} \right] \right] \\
 & \sqrt{w2 + w4} \cdot \left[0.5 \cdot \left[\begin{matrix} dFm_t & dPWm_t \end{matrix} \right] \right] \\
 & \sqrt{w3 + w4} \cdot \left[0.5 \cdot \left[\begin{matrix} dPRIm_t & dPWm_t \end{matrix} \right] \right] \\
 & \sqrt{w2} \cdot dFm_t \\
 & \sqrt{w3} \cdot dPRIm_t \\
 & \sqrt{w4} \cdot dPWm_t
 \end{aligned}$$

Side lobes Probability of identification matrix:

(g-20)

$P_{is} := \max_t$

$$\begin{aligned}
 & 1 \cdot \left[0.25 \cdot \left[\begin{matrix} dAOAs_t & dFs_t & dPRIs_t & dPWs_t \end{matrix} \right] \right] \\
 & \sqrt{w1 + w2 + w3} \cdot \left[0.333 \cdot \left[\begin{matrix} dAOAs_t & dFs_t & dPRIs_t \end{matrix} \right] \right] \\
 & \sqrt{w1 + w2 + w4} \cdot \left[0.333 \cdot \left[\begin{matrix} dAOAs_t & dFs_t & dPWs_t \end{matrix} \right] \right] \\
 & \sqrt{w1 + w3 + w4} \cdot \left[0.333 \cdot \left[\begin{matrix} dAOAs_t & dPRIs_t & dPWs_t \end{matrix} \right] \right] \\
 & \sqrt{w2 + w3 + w4} \cdot \left[0.333 \cdot \left[\begin{matrix} dFs_t & dPRIs_t & dPWs_t \end{matrix} \right] \right] \\
 & \sqrt{w1 + w2} \cdot \left[0.5 \cdot \left[\begin{matrix} dAOAs_t & dFs_t \end{matrix} \right] \right] \\
 & \sqrt{w1 + w3} \cdot \left[0.5 \cdot \left[\begin{matrix} dAOAs_t & dPRIs_t \end{matrix} \right] \right] \\
 & \sqrt{w1 + w4} \cdot \left[0.5 \cdot \left[\begin{matrix} dAOAs_t & dPWs_t \end{matrix} \right] \right] \\
 & \sqrt{w2 + w3} \cdot \left[0.5 \cdot \left[\begin{matrix} dFs_t & dPRIs_t \end{matrix} \right] \right] \\
 & \sqrt{w2 + w4} \cdot \left[0.5 \cdot \left[\begin{matrix} dFs_t & dPWs_t \end{matrix} \right] \right] \\
 & \sqrt{w3 + w4} \cdot \left[0.5 \cdot \left[\begin{matrix} dPRIs_t & dPWs_t \end{matrix} \right] \right] \\
 & \sqrt{w2} \cdot dFs_t \\
 & \sqrt{w3} \cdot dPRIs_t \\
 & \sqrt{w4} \cdot dPWs_t
 \end{aligned}$$

The Probability of identification vs. time is written into an output file:

WRITEPRN $\begin{bmatrix} \text{PidmIFM} \\ \text{prn} \end{bmatrix} := \text{Pim}_t$

WRITEPRN $\begin{bmatrix} \text{PidsIFM} \\ \text{prn} \end{bmatrix} := \text{Pis}_t$

APPENDIX H: PROBABILITY OF COINCIDENCE (SUPERHET)

Superhet Receiver case

This file calculates the probability of coincidence for a Superhet ESM - Frequency hopper (pulse to pulse) Radar type of encounter based on the theory explained in Wiley's book, that is considering an approach using window functions.

```
Radar := READPRN [ Radar  
                  prn ]
```

```
ESM := READPRN [ ESM  
                 prn ]
```

RADAR PARAMETERS

```
hr := Radar  
    0  
Pt := Radar  
    1  
ft := Radar  
    2  
 $\lambda$  := Radar  
    3  
Gtml := Radar  
    4  
Gtsl := Radar  
    5  
PRF := Radar  
    6  
PRI := Radar  
    7  
PW := Radar  
    8  
g := Radar  
    9  
B3dB := Radar  
    10  
Ta := Radar  
    11  
ra := Radar  
    12  
Lt := Radar  
    13
```

ESM RECEIVER PARAMETERS

Vmph := ESM
 0
 Vm := ESM
 1
 hesm := ESM
 2
 FL := ESM
 3
 FU := ESM
 4
 D := ESM
 5
 Br := ESM
 6
 Bv := ESM
 7
 Ba := ESM
 8
 Γ := ESM
 9
 gamma := ESM
 10
 PG := ESM
 11
 Fn := ESM
 12
 FN := ESM
 13
 Gesm := ESM
 14
 Pfa := ESM
 15
 Lesm := ESM
 16
 Ts := ESM
 17
 τf := ESM
 18
 d := ESM
 19
 T := ESM
 20
 tf := ESM
 21

Range Calculations

$$ae := 8493.3 \cdot 10^3 \quad \text{Earth Radius (m)}$$

$$t := 0, 1 \dots tf$$

$$t1_t := T \cdot t \quad hr_{Km} := \frac{hr}{1000} \quad hesm_{Km} := \frac{hesm}{1000}$$

$$R1 := ae + hr$$

$$R2 := ae + hesm$$

Maximum Range (Radar Horizon):

$$Rmax := 130.34 \cdot 10^3 \cdot \left[\sqrt{\frac{hesm}{Km}} + \sqrt{\frac{hr}{Km}} \right] \quad (h-1)$$

Maximum Range Angle:

$$\theta_{rad} := \arccos \left[\frac{R_{max}^2 - R1^2 - R2^2}{-2 \cdot R1 \cdot R2} \right] \quad (h-2)$$

Range Angle Increment:

$$\theta_t := \left[\begin{array}{c} t1 \\ Vm \cdot \frac{t}{R1} \end{array} \right] \quad (h-3)$$

LOS Range Increment:

$$R_t := \sqrt{R1^2 + R2^2 - [2 \cdot R1 \cdot R2 \cdot \cos[\theta_{rad} - \theta_t]]} \quad (h-4)$$

PROBABILITY OF COINCIDENCE CALCULATIONS

$$n := 5 \quad \text{Number of frequencies hopped over} \quad (h-5)$$

$$\tau_1 := \tau_a - d \quad (h-6) \quad \tau_4 := 2 \cdot PW - d \quad (h-7)$$

$$\tau_2 := \tau_f - d \quad (h-8) \quad \tau_{11} := (\tau_a - \tau_a) - d \quad (h-9)$$

$$\tau_3 := PW - d \quad (h-10) \quad \text{Thop} := n \cdot PRI \quad (h-11)$$

Mean time between coincidences:

$$T_{om} := \frac{\tau_a \cdot \tau_s \cdot PRI \cdot \text{Thop}}{\tau_1 \cdot \tau_2 \cdot \tau_3 + \tau_1 \cdot \tau_2 \cdot \tau_4 + \tau_1 \cdot \tau_3 \cdot \tau_4 + \tau_2 \cdot \tau_3 \cdot \tau_4} \quad (h-12)$$

$$T_{os} := \frac{\tau_a \cdot \tau_s \cdot PRI \cdot \text{Thop}}{\tau_{11} \cdot \tau_2 \cdot \tau_3 + \tau_{11} \cdot \tau_2 \cdot \tau_4 + \tau_{11} \cdot \tau_3 \cdot \tau_4 + \tau_2 \cdot \tau_3 \cdot \tau_4} \quad (h-13)$$

Instantaneous Coincidence Probability:

$$P_{om} := \frac{\tau_1 \cdot \tau_2 \cdot \tau_3 \cdot \tau_4}{\tau_a \cdot \tau_s \cdot PRI \cdot \text{Thop}} \quad (h-14)$$

$$P_{os} := \frac{\tau_{11} \cdot \tau_2 \cdot \tau_3 \cdot \tau_4}{\tau_a \cdot \tau_s \cdot PRI \cdot \text{Thop}} \quad (h-15)$$

$$K_m := 1 - P_{om} \quad (h-16) \quad K_s := 1 - P_{os} \quad (h-17)$$

Probability of Coincidence vs. Time:

$$P_{cm1}_t := 1 - \left[K_m \cdot \exp \left[\max \left[\frac{-t_1}{t} \right] \right] \right] \quad (h-18)$$

$$P_{cs1}_t := 1 - \left[K_s \cdot \exp \left[\max \left[\frac{-t_1}{t} \right] \right] \right] \quad (h-19)$$

Probability of coincidence vs. time is written into an output file:

WRITEPRN $\left[\begin{matrix} P_{cmhop} \\ prn \end{matrix} \right] := P_{cm1}_t$

WRITEPRN $\left[\begin{matrix} P_{cshop} \\ prn \end{matrix} \right] := P_{cs1}_t$

APPENDIX I: PROBABILITY OF COINCIDENCE (IFM)

IFM Receiver case

This file calculates the probability of coincidence for an IFM based ESM-Radar type of encounter based on the theory explained in Wiley's book, and in Self's article [Refs. 2 and 12] that is, considering an approach using window functions.

```
Radar := READPRN [Radar  
                  prn ]
```

```
ESMifm := READPRN [ESMifm  
                  prn ]
```

RADAR PARAMETERS

```
hr := Radar  
    0  
Pt := Radar  
    1  
ft := Radar  
    2  
 $\lambda$  := Radar  
    3  
Gtml := Radar  
    4  
Gtsl := Radar  
    5  
PRF := Radar  
    6  
PRI := Radar  
    7  
PW := Radar  
    8  
g := Radar  
    9  
B3dB := Radar  
    10  
Ta := Radar  
    11  
 $\tau_a$  := Radar  
    12  
Lt := Radar  
    13
```

ESM RECEIVER PARAMETERS

```

Vmph := ESMifm
      0
Vm := ESMifm
    1
hesm := ESMifm
    2
FL := ESMifm
    3
FU := ESMifm
    4
D := ESMifm
    5
Br := ESMifm
    6
Bv := ESMifm
    7
Ba := ESMifm
    8
Γ := ESMifm
    9
gamma := ESMifm
      10
PG := ESMifm
    11
Fn := ESMifm
    12
FN := ESMifm
    13
Gesm := ESMifm
      14
Pfa := ESMifm
      15
Lesm := ESMifm
      16
d := ESMifm
    17
T := ESMifm
    18
tf := ESMifm
    19

```


Range Calculations

$$ae := 8493.3 \cdot 10^3 \quad \text{Earth Radius (m)}$$

$$t := 0,1 \dots tf$$

$$t1_t := T \cdot t \quad hr_{Km} := \frac{hr}{1000} \quad hesm_{Km} := \frac{hesm}{1000}$$

$$R1 := ae + hr$$

$$R2 := ae + hesm$$

Maximum Range (Radar Horizon):

$$Rmax := 130.34 \cdot 10^3 \cdot \left[\sqrt{\frac{hesm}{Km}} + \sqrt{\frac{hr}{Km}} \right] \quad (i-1)$$

Maximum Range Angle:

$$\theta_{rad} := \arccos \left[\frac{Rmax^2 - R1^2 - R2^2}{-2 \cdot R1 \cdot R2} \right] \quad (i-2)$$

Range Angle Increment:

$$\theta_t := \left[\frac{t1_t}{Vm \cdot R1} \right] \quad (i-3)$$

LOS Range Increment:

$$R_t := \sqrt{R1^2 + R2^2 - [2 \cdot R1 \cdot R2 \cdot \cos[\theta_{rad} - \theta_t]]} \quad (i-4)$$

PROBABILITY OF COINCIDENCE CALCULATIONS

$n := 5$ Number of frequencies to be hopped over (i-5)

$\tau_1 := \tau_a - d$ (i-6) $\tau_3 := 2 \cdot PW - d$ (i-7)

$\tau_2 := PW - d$ (i-8) $Thop := n \cdot PRI$ (i-9)

$\tau_{11} := (Ta - 10 \cdot \tau_a) - d$ (i-10)

Mean time between coincidences:

$T_{om} := \frac{Ta \cdot Thop \cdot PRI}{\tau_1 \tau_2 + \tau_1 \cdot \tau_3 + \tau_2 \cdot \tau_3}$ Main lobe (i-11)

$T_{os} := \frac{Ta \cdot Thop \cdot PRI}{\tau_{11} \cdot \tau_2 + \tau_{11} \cdot \tau_3 + \tau_2 \cdot \tau_3}$ Side lobe (i-12)

Instantaneous Coincidence Probability:

$P_{om} := \frac{\tau_1 \cdot \tau_2 \cdot \tau_3}{Ta \cdot Thop \cdot PRI}$ Main lobe (i-13)

$P_{os} := \frac{\tau_{11} \cdot \tau_2 \cdot \tau_3}{Ta \cdot Thop \cdot PRI}$ Side lobe (i-14)

$K_m := 1 - P_{om}$ (i-15)

$K_s := 1 - P_{os}$ (i-16)

Probability of Coincidence vs. Time:

$$P_{cm11FM_t} := 1 - \left[K_m \cdot \exp \left[\max \left[\frac{-t1}{t} \right] \right] \right] \quad \text{Mainlobe} \quad (i-17)$$

$$P_{cs11FM_t} := 1 - \left[K_s \cdot \exp \left[\max \left[\frac{-t1}{t} \right] \right] \right] \quad \text{Sidelobe} \quad (i-18)$$

Probability of coincidence vs. time is written into an output file:

WRITEPRN $\left[P_{cm11FM_{prn}} \right] := P_{cm11FM_t}$

WRITEPRN $\left[P_{cs11FM_{prn}} \right] := P_{cs11FM_t}$

APPENDIX J; PROBABILITY OF INTERCEPT

This file reads all other probability files and calculates the final Probability of Intercept as function of time, $POI(t)$, for various conditions.

GET THE ITERATION TIME AND STEP SIZE:

ESM := READPRN [ESM
 prn]

ESMifm := READPRN [ESMifm
 prn]

T := ESM
 20

tf := ESM
 21

t := 0, 1 .. tf

t1 := t · T
 t

1.- READ ALL THE OTHER FILES

a.) Superhet files:

Pdgm := READPRN [Pdgm
 prn]

Pdgs := READPRN [Pdgs
 prn]

Pcmhop := READPRN [Pcmhop
 prn]

Pcshop := READPRN [Pcshop
 prn]

Pidm := READPRN [Pidm
 prn]

Pids := READPRN [Pids
 prn]

b.) IFM files:

$$\begin{aligned}
 P_{dgmIFM} &:= \text{READPRN} \left[\begin{array}{c} P_{dgmIFM} \\ \text{prn} \end{array} \right] & P_{dgsIFM} &:= \text{READPRN} \left[\begin{array}{c} P_{dgsIFM} \\ \text{prn} \end{array} \right] \\
 P_{cmIFM} &:= \text{READPRN} \left[\begin{array}{c} P_{cmIFM} \\ \text{prn} \end{array} \right] & P_{csIFM} &:= \text{READPRN} \left[\begin{array}{c} P_{csIFM} \\ \text{prn} \end{array} \right] \\
 P_{dmIFM} &:= \text{READPRN} \left[\begin{array}{c} P_{dmIFM} \\ \text{prn} \end{array} \right] & P_{dsIFM} &:= \text{READPRN} \left[\begin{array}{c} P_{dsIFM} \\ \text{prn} \end{array} \right]
 \end{aligned}$$

2.- PROBABILITY OF INTERCEPT FOR A SUPERHET RECEIVER:

a.) Probability of Intercept (Mainlobe):

$$P_{Olgm}_t := P_{dgm}_t \cdot P_{cmhop}_t \cdot P_{idm}_t \quad (j-1)$$

b.) Probability of Intercept (Sidelobes):

$$P_{Olgs}_t := P_{dgs}_t \cdot P_{cshop}_t \cdot P_{ids}_t \quad (j-2)$$

c.) Overall Probability of Intercept (Superhet Receiver):

$$P_{Olg}_t := P_{Olgm}_t + P_{Olgs}_t - P_{Olgm}_t \cdot P_{Olgs}_t \quad (j-3)$$

3.- PROBABILITY OF INTERCEPT FOR AN IFM BASED RECEIVER:

a.) Probability of Intercept (Mainlobe):

$$P_{Olfmm}_t := P_{dgmIFM}_t \cdot P_{cmIFM}_t \cdot P_{dmIFM}_t \quad (j-4)$$

b.) Probability of Intercept (Sidechannel):

$$POI_{ifs_t} := PdgsIFM_t \cdot PcsIFM_t \cdot PidsIFM_t \quad (j-5)$$

c.) Overall Probability of Intercept (IFM Receiver):

$$POI_{ifm_t} := POI_{ifmm_t} + POI_{ifs_t} - [POI_{ifmm_t} \cdot POI_{ifs_t}] \quad (j-6)$$

LIST OF REFERENCES

1. LCDR. Butcher M. USN, "Fighting the PHM's", *Proceedings U. S. Naval Institute*, April 1989.
2. Wiley R., *Electronic Intelligence; The Interception of Radar Signals*, Artech House, Norwood MA., 1985.
3. Tsui J. B., *Microwave Receivers with Electronic Warfare Applications*, John Wiley & Sons Inc., 1986.
4. Skolnik M., *Introduction to Radar Systems*, McGraw-Hill, 1980.
5. Lemley L. W., *Computers/Processors (for Electronic Warfare)*, NRL Report #247, Naval Research Laboratory, Washington D. C., August 1978.
6. Wilson L., *Introduction to ESM Preprocessors*, Classnotes, Naval Postgraduate School, Monterey California, 1978.
7. Glenn A. B., "Electronic Warfare Measure of Effectiveness", *IEEE 1981 International Conference on Communications*, 36, 6, 1-5, Denver CO. Vol. 2. 14-18, June 1981. IEEE, Piscataway, NJ.

8. Murry H., "100 Percent Probability of Intercept?". *Defense Electronics*, February 1986.
9. Ortiz J., *Mathematical Study for Predicting the Probability of Intercept for Airborne Radars*, Master's Thesis, Naval Postgraduate School, Monterey, California, September 1988.
10. Giaquinto J., *Computer-Aided Mathematical Analysis for Determining Intercept Time and Intercept Probability for Airborne Radars by Electronic Surveillance Measure Receivers*, Master's Thesis, Naval Postgraduate School, Monterey, California, June 1989.
11. Hoisington D. B., *Electronic Warfare*, Classnotes, Naval Postgraduate School, Monterey, California, 1978.
12. Wiley R., *Electronic Intelligence: The Analysis of Radar Signals*, Artech House, Norwood MA., 1982.
13. Self A. G., "Intercept Time and Its Prediction", *Journal of Electronic Defense*, August 1983.
14. Davies C. L., "Automatic Processing for ESM", *IEEE Proceedings*, Vol.129, Pt. F, No.3, p.164-171, June 1982.

DISTRIBUTION LIST

1. Defense Technical Information Center 2
Cameron Station
Alexandria, Virginia 22305-6145
2. Library, Code 0142 2
Naval Postgraduate School
Monterey, California 93943-5002
3. Direccion General de Educacion 1
Primera Zona Naval
Guayaquil, Ecuador
4. Naval Postgraduate School 2
Attn: Captain Thomas H. Hoivik, Code 55 Ho
Monterey, California 93943
5. Naval Postgraduate School 2
Attn: Robert L. Partelow, Code 62 Pw
Monterey, California, 93943
6. TNFG-UN Oswaldo Rosero Q. 2
Villavicencio 2300 y El Oro
Guayaquil, ECUADOR